ABSTRACT

ELECTRICAL RESISTIVITY OF ALUMINUM ALLOYS
AT LOW TEMPERATURES

By

Ronald Leon Carter

The electrical resistivities of aluminum and alloys of aluminum with magnesium, copper, zinc, or gallium have been measured from 2.5°K to 300°K. The importance of corrections for change in volume upon alloying and thermal expansion in determining the magnitude and temperature derivative of deviations from Matthiessen's Rule at high temperatures is stressed. Two hypotheses were found to be consistent with the deviations from Matthiessen's Rule measured at low temperatures. The conclusion that the electron states on the third zone sheet of the Fermi surface have an average relaxation time which is considerably different from that for the hole states on the second sheet was drawn from the application of the two-band model. The relative resistivities of the two bands, $\rho_{ph}^{e} > \rho_{ph}^{h}$, were shown to be consistent with thermoelectric power data. The data were also found to be consistent with a theory due to Mills, which considers the additional resistivity for a process which involves simultaneous scattering from an impurity ion and the emission or absorption of a phonon.

ELECTRICAL RESISTIVITY OF ALUMINUM ALLOYS AT LOW TEMPERATURES

By

Ronald Leon Carter

A THESIS

Submitted to
Michigan State University
in partial fulfillment of the requirements
for the degree of

DOCTOR OF PHILOSOPHY

Department of Physics

1971

ACKNOWLEDGMENTS

I would like to express my appreciation to Professor Frank J. Blatt, who first suggested this study, and whose advice and assistance on theoretical and experimental matters was invaluable and cheerfully offered. And to Professor Peter A. Schroeder, who heard many tales of woe and experimental failure, thank you for your freely offered help. I also acknowledge Professors Blatt and Schroeder and the National Science Foundation for financial support received during this study.

I would like to acknowledge Professor Carl L. Foiles for his work in doing the resistivity at high pressure measurements which were useful in the analysis of this study, and for many helpful discussions on transport measurements. Thanks are due also to Professor W.M. Hartmann for providing the results of his phonon dispersion calculations for aluminum before publication.

The efforts of Professors B.H. Wildenthal and W.H. Kelly in providing computer time on the XDS Sigma Seven are greatly appreciated for the time their efforts saved for me.

I would like to acknowledge the help of Mr. J. Thomas and Miss G. Pucilowski in setting up the computer programs, and to Miss Pucilowski for doing the drawings.

I am pleased to also acknowledge the help of Mr. B. Shumaker in the manufacture of some of the alloy samples.

My deepest appreciation is for my wife, Carole, who accepted many things that were less than they might be, offered encouragement when needed, typed this manuscript, and who worked very hard to make this study possible.

TABLE OF CONTENTS

LIST OF TABLES

LIST OF FIGURES

INTRODUCTION

Matthiessen's Rule

More than a century ago, Matthiessen (1,2) observed that near room temperature the temperature derivative of the resistivity of a dilute metal alloy is the same as for the pure base metal. Thus, the Matthiessen Rule (MR) is,

$$\frac{d\rho_P}{dT} = \frac{d\rho_A}{dT} \qquad 1.1$$

where T is the absolute temperature, and ρ_P and ρ_A are the resistivities of the pure metal and alloy respectively.

When temperatures near the absolute zero became experimentally attainable, it was observed that the limiting behavior of a "perfectly pure" metal was

$$\rho_P(T=0) = 0, \qquad 1.2$$

and for an alloy

$$\rho_A(T=0) = \rho_o. \qquad 1.3$$

Where ρ_o, the residual resistivity, appears in the integrated form of the MR:

$$\rho_A = \rho_P + \rho_o. \qquad 1.4$$

When Bloch (3,4) and later Grüneisen (5), formulated early theories of the effect of the thermal motion of the ions (phonons) on the electrical resistivity of a pure metal, ρ_p was identified as ρ_{ph}, the resistivity due to scattering of the electrons by the phonons. The residual resistivity, ρ_o, was then identified as due to scattering of the electrons by imperfections in the lattice. Thus, the MR was given the more general interpretation: the partial resistivities arising from the scattering of the conduction electrons by different types of scatterers are additive.

Deviations from Matthiessen's Rule

In practice, deviations from the MR are usually observed in dilute metal alloys. The temperature dependence of the alloy resistivity is not identical to the temperature dependence of the pure resistivity. Thus,

$$\rho_A^{(T)} = \rho_{ph}^{(T)} + \rho_o + \Delta(T), \qquad 1.5$$

where $\Delta(T)$, the deviation from the MR, depends on the nature and concentration of defects and impurities in a complex manner.

Departures from the MR can arise for a number of reasons. Some of the most important (for nonmagnetic impurities) are:

Δ_1: The addition of impurities may change the phonon spectrum of the metal.

Δ_2: The electronic band structure may be altered by the impurity.

Δ_3: Scattering from the thermally oscillating impurities may give a temperature dependent impurity resistivity (phonon-assisted impurity scattering).

Δ_4: Interference terms between scattering by the vibrating impurities and the host ions.

Δ_5: Two (or more) groups of electrons may contribute to the conductivity, giving (as will be shown later) an apparent deviation from the MR.

Δ_6: The simultaneous presence of thermally induced Umklapp processes and impurity scattering.

In this study, dilute alloys were considered; the maximum impurity content being less than two atomic per cent (2 a/o). In this case, de Haas-van Alphen measurements (6) support the assumption that changes in the electronic band structure are negligible. Furthermore, the results of Mössbauer experiments (7,8) indicate that the phonon spectrum is little changed.

Extensive reviews of the theoretical and experimental work on departures from the MR have been given by Lengler, Schilling and Wenzl (9), Stewart and Huebener (10),

and Seth and Woods (11). A brief discussion of the theoretical points important to this study follows.

Kagan and Zhernov (12) have developed a theory of the electrical resistivity of a metal with impurities which takes into account deformation of the phonon spectrum due to the presence of the impurity ions and the electron scattering by the thermally oscillating impurity ions. In the low temperature range, scattering by the oscillating impurity ions gives a term proportional to $\rho_o T^2$, interference between scattering by the perturbed phonon spectrum and the oscillating impurity ion gives a term proportional to $\rho_o T^4$, and scattering by the deformed phonon spectrum gives a term proportional to $\rho_o T^5$. The temperature variation was shown to exhibit an anomaly in the case of heavy impurity atoms when a quasilocal level appears in the phonon spectrum. At high temperatures, the impurity part of the resistivity was shown to vary linearly with temperature, the sign of the derivative depending on the relative positions of the impurity (solute) and matrix (solvent) atoms in the periodic table.

A theory for the phonon-assisted impurity scattering due to the average strain induced in the lattice by the thermally oscillating impurity atoms has been formulated by Klemens (13). Assuming the change in the impurity potential to be proportional to strain, Klemens showed the additional resistivity to be proportional to $\rho_o \langle \varepsilon^2 \rangle$. The

mean-square thermal strain of the lattice, $\langle\varepsilon^2\rangle$, is proportional to the thermal vibrational energy of the lattice, so $\Delta_3 \propto \rho_o T^4 (T << \theta_D)$, and $\Delta_3 \propto \rho_o T (T \gtrsim \theta_D)$.

Ehrlich (14) has calculated the low temperature resistivity for the case for which the Fermi surface touches or nearly touches the Brillouin zone boundaries, extending the Klemens-Jackson (15) theory to include the simultaneous presence of impurity and thermally induced umklapp scattering. Assuming an isotropic, temperature independent, impurity relaxation time, Ehrlich solved the Boltzmann equation in terms of a Legendre series in the scattering angle for current-carrying electrons. For the case in which the phonon resistivity, ρ_{ph}, in the absence of umklapp processes is proportional to T^5, the numerical solution for the total resistivity is of the form

$$\rho(T) = \rho_o + a(P,\varepsilon)T^2 + b(P,\varepsilon)T^5 \qquad 1.6$$

where $P = 2\rho_o/\rho_{ph}$ and ε is the angle of contact of the Fermi surface on the Brillouin zone. The combined effect of impurity and umklapp scattering processes introduces a T^2 term as well as enhancing the T^5 term.

Mills (16) has calculated the resistivity for a process which involves simultaneous scattering from an impurity ion and the emission or absorption of a phonon. Breakdown of momentum conservation leads to a T^3 dependence for this resistive contribution. Further, as a result

of the small energy difference between initial and intermediate states for the process, this contribution to Δ_4 is weakly dependent on the impurity concentration.

Dugdale and Basinski (17) interpreted the results of measurements on copper and gold based alloys using a simple two-band model. Originally proposed by Sondheimer and Wilson (18) and Kohler (19) the two-band model approximates anistropies of the relaxation times associated with phonon and impurity scattering with two non-interacting conduction bands with isotropic relaxation times.

Deviations from Matthiessen's Rule in Aluminum

Aluminum was chosen for this study of deviations from the MR for three reasons. First, there is reason to suspect *a priori* that the sources for deviations Δ_3, Δ_4, Δ_5, and Δ_6 should be manifest in aluminum alloys. Second, the cubic symmetry of the face-centered cubic aluminum lattice permitted the use of wire resistance samples. Last, deviations from the MR had been previously reported in aluminum systems (11, 20-24).

The light aluminum ions should experience rather large amplitude thermal vibrations, so the scattering effects of thermal strain at impurity sites might be expected to be pronounced. The relatively light mass of the aluminum ion should favor creation of in-band local modes or quasilocal levels in the phonon spectrum upon alloying

with heavy solutes. This might be expected to give the anomalous impurity resistivity anticipated by Kagan and Zhernov (12). The reversal of the Hall field in pure aluminum reported by Lück (25) and Forsvoll and Holwech (26) from the low field electron-like limit to the high field hole-like limit supports the hypothesis that aluminum may be treated as a two-band metal. With this hypothesis, the Kohler-Sondheimer-Wilson equation (18,19) may be used to fit the deviations, Δ_5, from the MR, and thus infer the relative relaxation times for scattering by impurities and phonons for electrons in the two bands.

Alley and Serin (20) have reported departures from the MR in alloys of aluminum with zinc, magnesium, germanium, or silver from 4.2 to 300°K. This work did not include dimensional measurements, so deviations could only be inferred and not quantitatively compared with theory. Van Zytveld and Bass (21) have carefully documented size dependent deviations from the MR in thin foils and fine wires of aluminum from 1.3 to above 40°K. Panova, Zhernov and Kutaisev (22) have reported deviations from the MR in alloys of aluminum with gold or silver solutes from 4.2 to 300°K, interpreting their results on the basis of the Kagan and Zhernov (12) theory. Panova et al. did not, however, study the effects of change in valence or of light solutes. Recently, Seth and Woods (11) have reported deviations from the MR in alloys of aluminum with magnesium or silver

from 4.2 to 300°K. Caplin and Rizzuto (23) report deviations from the MR in alloys of aluminum with magnesium, iron, silicon, cobalt, manganese, copper, chromium, or vanadium. Campbell, Caplin and Rizzuto (24) later interpreted these deviations in light of the Mills theory (16).

In the following chapters, the deviations from Matthiessen's rule are reported for aluminum with magnesium, zinc, copper, or gallium solutes.

EXPERIMENTAL APPARATUS

Cryostat and Sample Mounting

The cryostat used was of the sample holder-within a cannister-within a vacuum jacket-within an outer cannister-design. A schematic representation of the cryostat is shown in Figure 1.

The sample holder was made of aluminum to minimize the effects of differential thermal expansion between the samples and the sample holder. The inner diameter of the hollow cylindrical sample holder was designed for a loose fit on the oxygen free high conductivity (OFHC) copper block (to minimize strains due to differential thermal expansion), with firm thermal contact insured by mechanically bolting the sample holder to the OFHC block at a single point. The outside of the sample holder was insulated by cigarette paper attached with GE 7031 Varnish. Samples were annealed in a coil slightly larger than the sample holder diameter, placed on the sample holder, and held in place by spring-loaded clamps. Thus, strains induced in the samples due to mounting or thermal cycling were minimized. Platinum and germanium resistance thermometers were mounted in the thermometer well in the interior of the OFHC copper block for measurement of the sample temperature.

LEGEND

F	Flange
BP	Binding Post (OFHC Copper)
HL	Heat Leak to Bath
S	Solder
PBO	Lead O-Ring

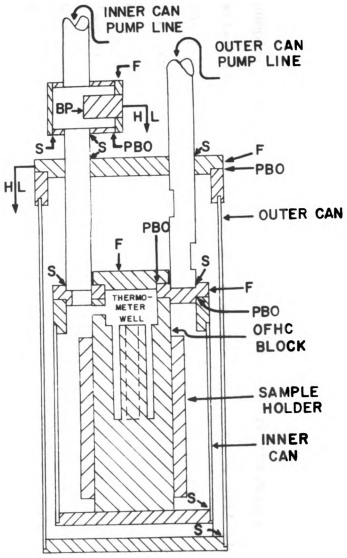

Figure 1.--Schematic representation of the cryostat.

Potential and current leads for the samples and thermometers were run through the stainless steel inner can pumping line. These B&S 38 copper wires were thermally attached to the OFHC copper block and the binding post in the pumping line (which was provided with a heat leak to the cryogenic liquid). A second variable heat leak could be provided by introducing exchange gas into the vacuum jacket between the inner and outer cannisters. Exchange gas could also be introduced into the vacuum space in the inner cannister.

Current Control

The sample and thermometer currents were held constant to better than .001% during the period of a measurement (about 30 minutes) using the constant current source shown in Figure 2. In this configuration, the operational amplifier output causes current to flow in the feed-back loop (the load, R1 and SR) and then through CR, with such a magnitude that the potential drop across CR matches the offset potential of the mercury cell, RM-42R. Variation of CR may then be used to adjust the load current, which may be measured by the potential drop across the standard resistor, SR.

The Analog Devices 118A is capable of supplying currents up to 5 mA. For the low temperature resistivity measurements, up to 100 mA was required. The current was boosted using transistor Q1 by breaking the feed-back loop

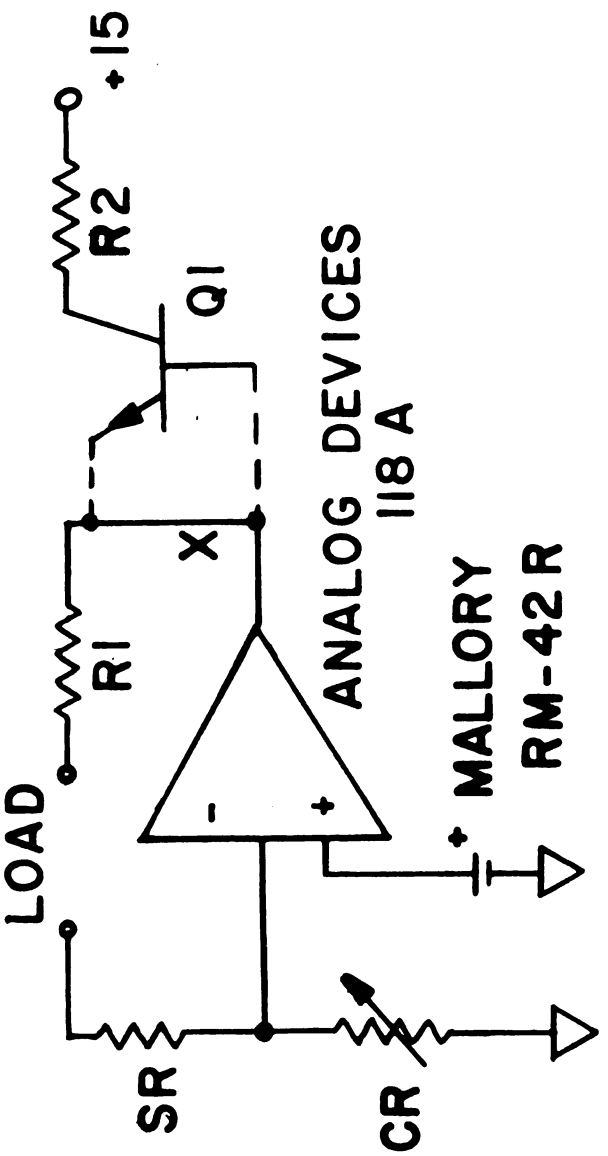

Figure 2.--Constant current source.

at X and making the connections shown in dashed lines. In this way, the available current was limited only by the power dissipation of Q1 and the +15 volt source.

Temperature Control

The temperature of the OFHC block was held constant to within .01°K during a 30 minute period by use of the temperature controller shown in Figure 3.

A Micro-Measurements Cryogenics Linear Temperature Sensor (CLTS) was mounted on the outer surface of the inner cannister with GE 7031 Varnish. The nominal resistance of the CLTS is 290Ω at 300°K and the sensitivity is nearly constant at .239Ω/°K down to 4°K. The CLTS is used as one arm of a bridge with the off-balance voltage amplified by an Analog Devices (AD) 118K. The AD 118A is connected in a standard differentiator-integrator control configuration. The control voltage of the AD 118A is converted to a phase-controlled pulse by the 2N1671B unijunction transistor circuit. Large control voltages generate a pulse early in the 60 cps line voltage half-cycle, while small control voltages cause a pulse later in the 60 cps line voltage half-cycle. These pulses are then applied to the gate of the RCA 40485 triac which then conducts for the remainder of the half-cycle. Since the triac is in series with a bifilar resistance heater wound on the outside of the outer cannister, the control voltage causes more or less

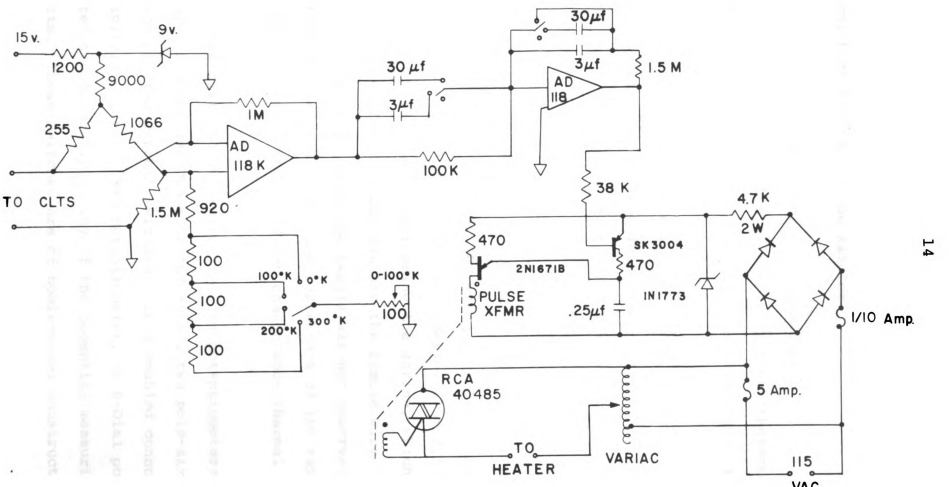

Figure 3.--Temperature controller.

average power to be put into the cryostat, causing heating or permitting cooling of the samples.

Potentiometric Measurements

The sample potentials, sample current, thermometer potentials, and thermometer current were measured in a circuit schematically represented in Figure 4. In practice, up to ten samples were connected in series for a given run. Copper potential and current leads were attached to the samples using the spring loaded system shown in Figure 5. The insulated washers were made by attaching cigarette paper to one side of a brass washer with GE 7031 Varnish. The insulating coating was removed from the end of the current or potential lead and the bared copper wire placed between the insulated washer and the sample. The nylon screw was then tightened compressing the spring, which then held the copper lead rigidly against the sample wire. Creeping of the lead along the sample was not observed, as inferred by the fact that the resistance of the sample at a specific temperature did not change upon thermal cycling.

The distribution switch for the potentiometers was made of three Chicago Dynamics Industries two pole-sixteen position printed circuit switches. This enabled connecting the digital voltmeter, K-3 potentiometer, or 6-Dial potentiometer independently to any of the potential measuring circuits. These switches are of noble-metal construction;

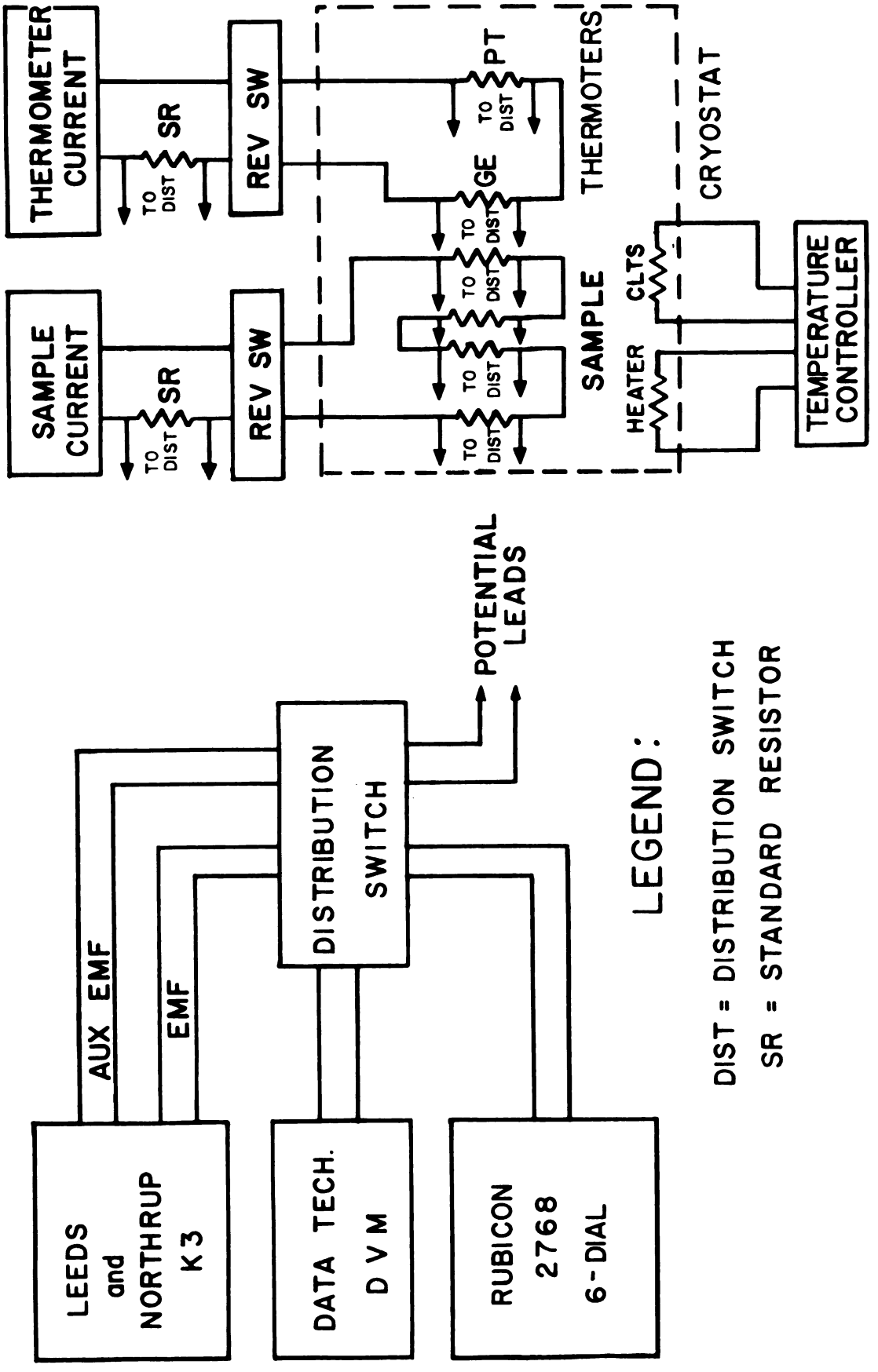

Figure 4.--Schematic representation of experimental apparatus.

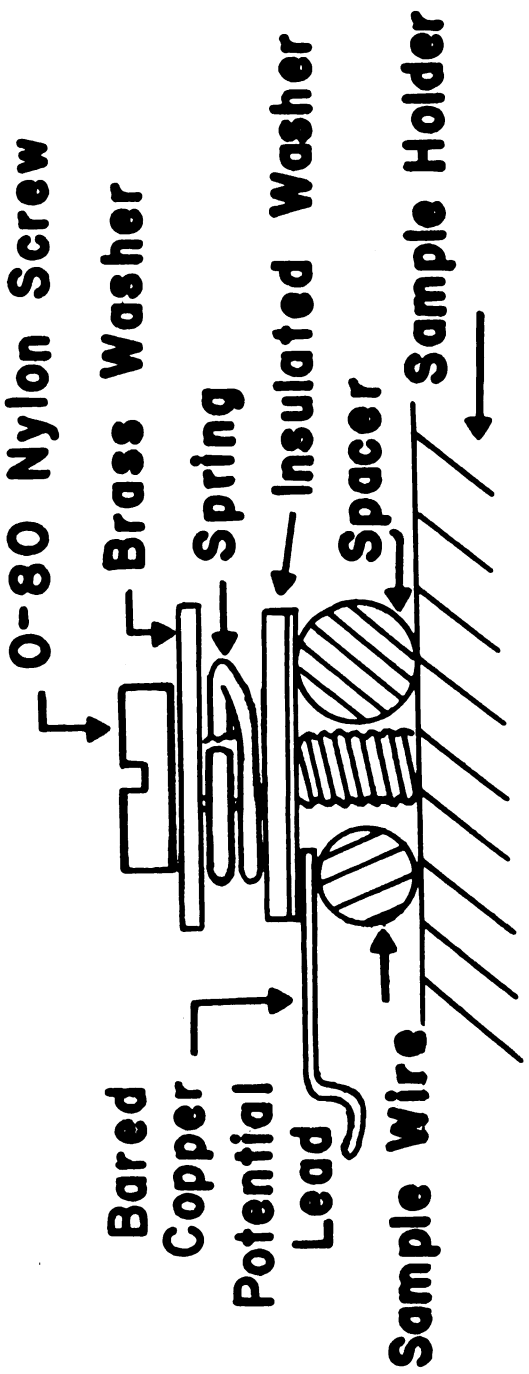

Figure 5.--Spring loaded electrical contacts.

and low thermal solder was used for all connections. Spurious thermal emfs observed upon reversal of the current were less than .02 μV.

The Leeds and Northrup K-3 potentiometer was used to measure the thermometer potentials and the potential drops across the standard resistors in the current supply circuits. The precision for this instrument is .015% or 2μV whichever is greater in the range used. The Rubicon 2768 6-Dial potentiometer was used to measure the potential drops across the samples. The precision for this instrument is .01% or .01μV whichever is larger in the range used.

SAMPLE PREPARATION

Manufacture of the Alloys

All of the alloys (except the Mg series) in this investigation were made from 6-9 grade aluminum, lot HPM 2404, purchased from Cominco American. The lot assay is shown in Table 1. The total impurity level was less than one part per million (ppm). A piece of lot HPM 2404 was also used for the pure aluminum sample, as well as some Gallard Schlesinger B 3015 zone refined aluminum. The doping level for the alloys ranged from .05 a/o (500 ppm) to 2 a/o. The doping material used was 5-9 or 6-9 grade material.

A master alloy (maximum concentration) for each series was made by R.F. induction melting the solute and solvent (pure aluminum) in a vitreous graphite crucible. After about two minutes of mixing by the stirring action of the induction heater, the molten alloy was poured into an aluminum chill-cast mold. A portion of the master alloy was melted and poured into the chill-cast mold a second time, for better mixing, and then used for the maximum concentration alloy. The remainder of the master alloy was further diluted with pure aluminum and chill-cast for the more dilute alloy samples. In some cases (as described

TABLE 1.--Lot assay for HPM 2404.

Impurity	Concentration (in ppm)
Ca	.1
Cn	.1
Fe	.3
Mg	.1
Mn	.3
Total	.9

below) chill-casting did not yield a homogeneous dopant concentration throughout the casting. These samples were given a homogenization period of one week at a temperature of about 550°C in an argon atmosphere.

The magnesium series of alloys was kindly provided in wire form by Dr. R. P. Huebener of the Argonne National Laboratory. Spectrographic analysis on the least concentrated alloy of the magnesium series revealed <10 ppm copper as the only detectable impurity. Electron microprobe analysis found copper and carbon present in amounts barely sufficient for detection (much less than 100 ppm).

Forming of Wires

The castings were removed from the chill-cast mold, a piece of the casting cut out and etched. This piece was then passed through a rolling mill until it formed a wire

of 1 mm square cross section. This wire was then drawn through tungsten carbide dies to 0.75 mm diameter. The final drawing operations were performed using diamond dies to a final diameter of 0.5 mm or 0.25 mm. After each pass through the rolling mill or dies the wires were carefully wiped clean using a lint-free tissue and ethyl alcohol. Sufficient time was allowed for the ethyl alcohol to evaporate before subsequent milling or drawing operations. The dies and rolling mill were also carefully cleaned with ethyl alcohol prior to use. Triple-distilled water was used if lubrication was needed during the drawing operations.

Resistance Ratios

For characterization of the samples, the resistivity ratio RR = R(295°K)/R(4.2°K), where R is the sample resistance, was found to be quite useful. The procedure was as follows: A piece of wire sample about 7 cm long was fixed with current and potential leads. This sample was placed in the room temperature resistivity apparatus and given time to come into thermal equilibrium with the apparatus. The resistance and temperature were then measured. Matthiessen's rule was assumed to calculate the resistance at 295°K. The sample was then placed in liquid helium and the resistance at 4.2°K was measured. The ratio RR, thus calculated, was then used in the characterization procedures. It should be noted that the resistance ratio thus found is not wholly accurate (since this investigation is

indeed founded on the experimental fact that Matthiessen's rule is not obeyed for aluminum alloys). This procedure can be properly used to infer the effect of annealing on residual resistivity and the homogeneity of alloy concentration along a wire, since a decrease or increase in RR, so defined, can be unequivocally used to infer a commensurate increase or decrease in the residual resistivity.

Annealing

A study of the effect of annealing on both pure and alloy samples revealed the following: No advantage could be found in annealing in an inert atmosphere as compared to air. All samples were therefore annealed in an aluminum foil "envelope" in air. After one hour of annealing at approximately 500°C, the residual resistivity decreased (as inferred by an increase in the resistance ratio) to within 1% of the minimum observed for a given sample. In the next one to two hours the minimum residual resistivity was observed to be reached. For further annealing no consistent variation was observed, until ten to twenty hours elapsed after which the residual resistivity began to increase. This was probably due to contamination from the air or aluminum foil. All samples were annealed in 10 cm diameter coils for two hours, then the room temperature resistivity was measured. The wire was then coiled to the diameter of the sample holder and given one more hour of annealing time. The resistivity ratio RR was observed to be constant to

within experimental error before and after the second anneal for all samples tested.

Sample Characterization

After formation into wires, and the initial two-hour anneal, the samples were tested by resistance-ratio, electron microprobe and chemical analysis to characterize the usefulness for this study.

A wire 90 cm in length was required for the resistivity measurements. Additional 10 cm lengths from each end were used for resistance ratio analysis. The sample was considered satisfactory for this study only if the resistance ratio of the two end pieces matched to within 5%. Furthermore, when installed in the cryostat, the sample from the central piece was required to have a resistance ratio within 3% of the average of the end pieces. This criterion was established to infer that fluctuations in alloy concentration of the samples used were about 3% of the average concentration. It was particularly difficult to achieve a sample with zinc, cadium, or silver as the solute which could pass this test. Even after one week of homogenization, only two zinc and one silver alloy samples were homogeneous enough to pass this test.

An Applied Research Laboratories electron microprobe was used to qualitatively analyze the least concentrated gallium and most concentrated copper samples for impurities. The electron microprobe is not suitable for

quantitative analysis of impurity levels below 300 ppm. However, it is possible to detect the presence of trace impurity levels to below 10 ppm. In addition to aluminum and the desired dopant, carbon, silicon, manganese, and copper were each observed at the threshold detection level. The lot analysis for the pure aluminum used included copper and manganese at below the 1 ppm level. It was assumed that carbon and silicon were picked up from the vitreous carbon crucible and vycor glass sleeve used in the melting operation.

Chemical analysis for the quantity of solute material was performed by Schwarzkopf Microanalytical Laboratories.

RESISTIVITY DATA

Introduction

The resistivities of pure aluminum and fourteen aluminum alloys were measured from 4.2°K (as low as 2°K in some cases) to 300°K. The specific resistivity of each sample was determined at room temperature. Resistances were measured for each sample as mounted in the cryostat as a function of temperature. These data were then converted to resistivities by normalization to the measured specific resistivity at room temperature.

Room Temperature Resistivity Measurements

The resistivity of a cylindrical wire sample of resistance R, length ℓ, and cross-sectional area A is given by

$$\rho = R \frac{A}{\ell}. \qquad 4.1$$

The resistivity of each wire sample used in this study was carefully determined at room temperature by measurement of the resistance per unit length and the mass, m, of a known length, ℓ, of wire. The area was calculated from the handbook value (27) for the density, d, according to the relationship

$$A = \frac{m}{d\ell_o}. \qquad 4.2$$

Each wire sample was placed on an Invar scale mounted in a channel milled out of a massive, thermally insulated, aluminum block. Razor blades were used for potential probes. Simultaneous position, potential, and current measurements were used to determine the resistance per unit length of the wire sample. The temperature was measured using a platinum resistance thermometer which was mounted in the aluminum block. Potentiometric measurements were made with the circuitry described under Experimental Apparatus, and shown in Figure 5. At the greatest length, ℓ_o, the razor blade potential probes were pressed down, cutting off ℓ_o of the wire. This amount of wire was weighed for its mass, m, using a Cahn microbalance (if microgram precision was required) or a Mettler model B-6 semi-micro balance. Corrections for the bouyancy of air were made when the Mettler Balance was used, but were not needed with the Cahn microbalance since the mass standards used were aluminum alloys within .3% of the density of the wire samples.

This procedure is applicable if the cross-sectional area is uniform along the entire length of the wire. To insure this, R/ℓ was measured as a function of the position along the wire. The variation in R/ℓ was assumed to be due to variation in A rather than alloy concentration. This

was assumed by the restrictions on the residual resistivity described previously.

If any part of the sample had a variation of R/ℓ of more than .03% from the mean, an alternate procedure was used. If the wire is supposed to be composed of segments ℓ_i in length with each segment A_i in cross-sectional area, the mass of the length, $\ell_o = n\ell_i$, of wire is

$$m = d\ell_i \sum_{i=1}^{n} A_i. \tag{4.3}$$

Now, since the resistance of each segment, R_i is

$$R_i = \rho \frac{\ell i}{A_i}. \tag{4.4}$$

The area of the segment may be inferred to be

$$A_i = \rho \frac{\ell i}{R_i} \tag{4.5}$$

giving

$$m = d\ell_i^{\,2} \rho \sum_{i=1}^{n} \frac{1}{R_i}. \tag{4.6}$$

Solving for the resistivity, we have

$$\rho = \frac{m}{d\ell_i^{\,2} \sum_{i=1}^{n} \frac{1}{R_i}}. \tag{4.7}$$

In practice, then, the wire was divided into n sections such that the values of R_i from adjacent sections varied by less than .03%, then R_i was measured for each ℓ_i and the resistivity calculated using the above expression.

Temperature Dependence of the Resistance

In practice, up to ten wire samples were connected in series in the cryostat for a given run. One of these samples was always pure aluminum. The data were taken in the sequence: potential for the pure aluminum sample (forward current), potential for alloy sample (forward current). thermometer potential, potential for alloy sample (reverse current), potential for pure aluminum sample (reverse current). In this way, the resistances of the alloy and pure aluminum were obtained for the same average temperature, minimizing the effect of uncertainty in temperature measurement.

The cryostat was immersed in or above liquid helium when taking data from 2°K to 65°K. The helium was pumped for data points below 4.2°K and temperature control achieved by regulation of the pumping speed. Good thermal contact with the bath was effected by introducing a small amount of helium gas into the inner and outer cannisters. For data points above 4.2°K, the outer cannister was pumped out and the temperature controller used to adjust the sample temperature and hold it constant.

The cryostat was immersed in liquid nitrogen when taking data above 65°K. In the range from 65°K to 77°K, the nitrogen was pumped and temperature control was achieved by regulation of the pumping speed. Helium gas was introduced into the inner and outer cannisters. For temperatures above 77°K, the outer cannister was evacuated and the temperature controller used to adjust the sample temperature and hold it constant.

Calculating the Resistivity from the Data

It is not sufficient over the entire range of temperature studied to simply normalize the resistance to the room temperature resistivity by using a temperature independent shape factor. Corrections must be made for change in volume due to thermal expansion and alloying.

Dugdale (17) has pointed out that deviations from Matthiessen's rule can be properly inferred only if the resistivities are all measured at the same atomic volume. The resistivity at a volume V was corrected for volume change to V_o by the relation

$$\rho(V_o) = \rho(v)\left[1 + \frac{V}{\rho}\frac{\partial\rho}{\partial V}\left(\frac{V_o - V}{V}\right)\right]. \qquad 4.8$$

The volume derivative may be calculated from the pressure derivative

$$\frac{V}{\rho}\frac{\partial \rho}{\partial V} = -\frac{1}{\rho}\frac{\partial \rho}{\partial P}\left(-\frac{1}{V}\frac{\partial V}{\partial P}\right)^{-1}, \qquad 4.9a$$

$$= -\frac{1}{\rho}\frac{\partial \rho}{\partial P}\frac{1}{\chi}, \qquad 4.9b$$

where χ is the compressibility of the sample material. The pressure derivative for the resistivity of an alloy may be separated into phonon and impurity resistivity terms. This is suggested by taking the pressure derivative of Matthiessen's rule.

$$\rho_t = \rho_{ph} + \rho_o \qquad 4.10$$

$$\frac{\partial \rho_t}{\partial P} = \frac{\partial \rho_{ph}}{\partial P} + \frac{\partial \rho_o}{\partial P} \qquad 4.11$$

Defining

$$\beta = -\frac{1}{\rho_{ph}}\frac{\partial \rho_{ph}}{\partial P}, \qquad 4.12$$

and

$$\gamma = -\frac{1}{\rho_o}\frac{\partial \rho_o}{\partial P}, \qquad 4.13$$

we have

$$\frac{1}{\rho_t}\frac{\partial \rho_t}{\partial P} = -\beta\frac{\rho_{ph}}{\rho_t} - \gamma\frac{\rho_o}{\rho_t}. \qquad 4.14$$

Bridgman (28) has measured the pressure derivative of aluminum between 90°K and 273°K. This data was extended to 4°K using the relation (29)

$$3\left[\frac{1}{\rho}\frac{\partial\rho}{\partial P}\right]_{\text{high T}} = \left[\frac{1}{\rho}\frac{\partial\rho}{\partial P}\right]_{\text{low T}}. \qquad 4.15$$

Bridgman (30) has also reported the pressure derivatives of the resistivity of Al-Mg and Al-Zn alloys at 273°K. Foiles (31) has measured the pressure derivative at 77°K of the Al-Mg alloys used in this investigation. For Al-Mg alloys, γ is $1.5(10^{-6})\text{cm}^2/\text{kg}$, and is independent of temperature. For Al-Zn alloys, γ is $-3.8(10^{-6})\text{cm}^2/\text{kg}$. For pure aluminum at 273°K, β is $4.03(10^{-6})\text{cm}^2/\text{kg}$.

Corrections were made to the resistivities following the two-step program suggested by Dugdale (17). First, ideal phonon resistivity, ρ_{ph}, has been corrected for volume dilatation on alloying. Thus

$$\rho_{ph}^{corr} = \rho_{ph}\left[1 + \frac{3\beta}{\chi}\left(\frac{a-a_o}{a_o}\right)\right], \qquad 4.16$$

where a_o and a are the lattice parameters of the pure material and the alloy respectively as reported by Pearson (27). Second, the residual resistivity of the alloy, ρ_o, has been corrected for the volume change due to thermal expansion. Thus

$$\rho_o(T) = \rho_o\left[1 + \frac{3\gamma}{\chi}(\alpha_o - \alpha)\right], \qquad 4.17$$

where α and α_o are the fractional linear expansion at temperature T and 0°K relative to 293°K as tabulated by Corruccini and Gniewek (32). The deviation from Matthiessen's rule at the temperature T is then

$$\Delta(T) = \rho_t(T) - \rho_o(T) - \rho_{ph}^{corr}. \qquad 4.18$$

Since γ was known for the Al-Mg and Al-Zn systems only, complete corrections have not been made for alloys in the Al-Cu, Al-Ga, and Al-Ag systems. The maximum error thus incurred is at high temperature. If we assume the γ value observed for Al-Zn is large, an approximate maximum for the correction is

$$\frac{3}{\chi}(\alpha_o - \alpha)\rho_o = \frac{3(3.8)(10^{-6})cm^2/kg(.00415)}{1.34(10^{-6})cm^2/kg}\rho_o \qquad 4.19a$$

$$= .045\ \rho_o. \qquad 4.19b$$

Consequently, for the Al-Cu, Al-Ga, and Al-Ag systems, it has been assumed uncertainties, $\delta\rho_{vol}$, due to volume corrections are

$$\delta\rho_{vol} \lesssim .05\ \rho_o. \qquad 4.20$$

A FORTRAN listing of a computer program used to calculate resistivities from the voltage data is shown in Appendix A. A typical data run computer output is in Appendix B. An error analysis is in Appendix C.

RESULTS AND CONCLUSIONS

The Phonon Resistivity of Aluminum

The temperature dependent resistivity, $\delta(T) = \rho(T) - \rho_o$, for three pure aluminum wire samples is shown as δ/T^2 vs T^3 in Figure 6. Reich (33) measured the resistivity of three samples from 14°K to 20°K. The power series fit to $\delta = aT^2 + bT^5$ obtained by Reich for ρ_o = .068 nΩ-cm sample is represented by a solid line in the region of data, and extended with a dashed line. On the basis of the data of Aleksandrov and D'yakov (34), Aleksandrov (35) proposed the fit shown as the dash-dot line in Figure 6. The coefficients a and b reported by Garland and Bowers (36), Reich (33), and Aleksandrov (35) and fit to the data of this investigation between 25°K and 40°K are summarized in Table 2. Below 25°K, the data deviates considerably from the straight line fit. This feature will be discussed later in terms of deviation from the MR. Above 45°K, the temperature dependence is weaker than T^5; eventually falling to a nearly linear functional behavior for temperatures above 100°K.

The Bloch-Grüneisen (3-5) theory for the resistivity due to phonon scattering predicts

$$\rho_{ph} \propto T^5, \quad T << \theta_D. \qquad 5.1$$

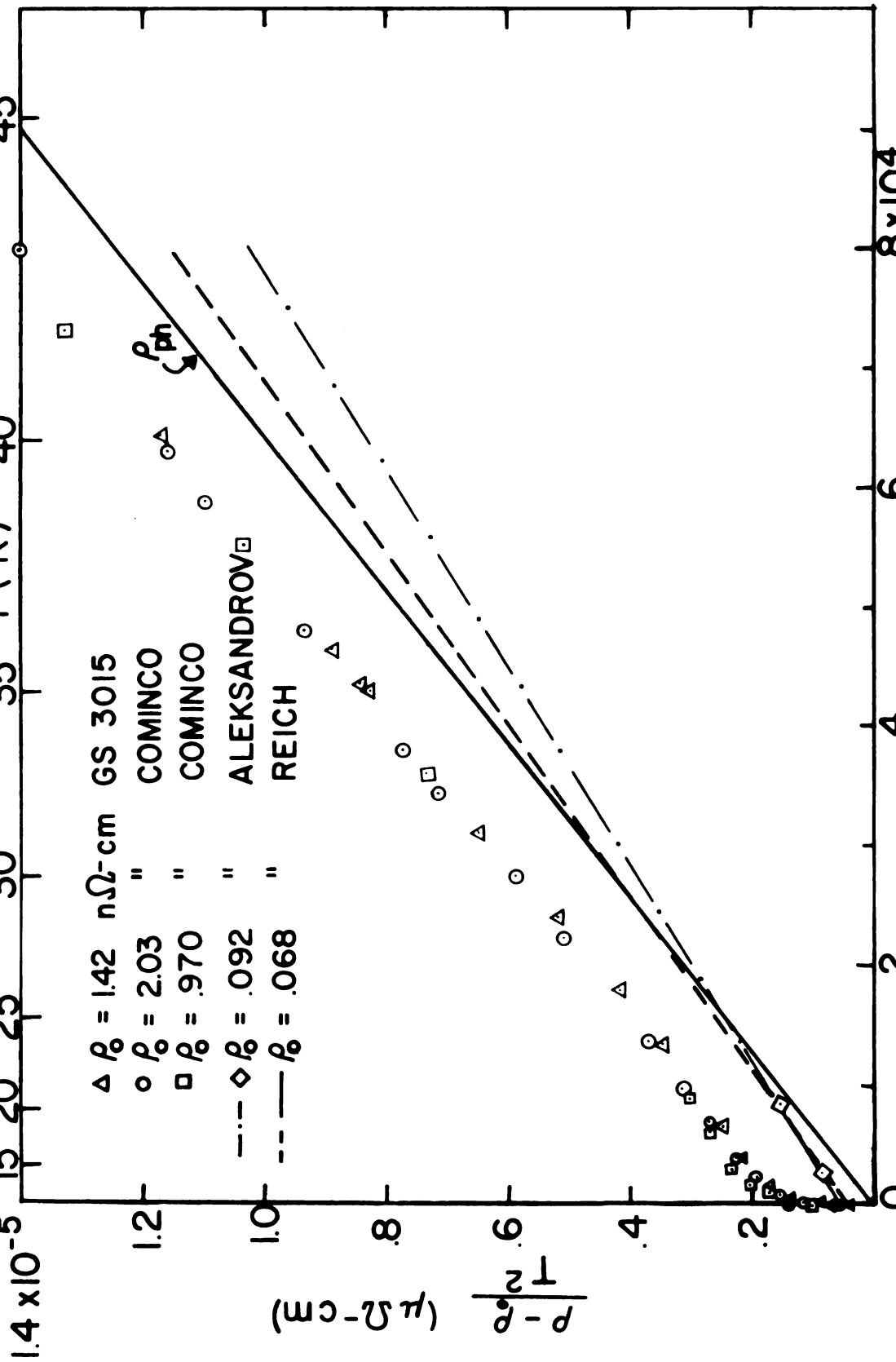

Figure 6.--Temperature dependent resistivity of pure aluminum.

TABLE 2.--Coefficients of the T^2 and T^5 components of the resistivity of aluminum.

Investigator	Wire Diameter (mm)	ρ_o (nΩ-cm)	$ax10^6$ (μΩ-cm/°K^2)	$bx10^{10}$ (μΩcm/°K^5)
Present Investigation	.50	1.42	1.25	1.56
Present Investigation	.25	2.03	1.50	1.46
Present Investigation	.25	.97	1.55	1.61
Garland & Bowers	1.05	1.04	0.44	
Reich	1.25	.22	0.64	1.18
Reich	5.22	.068	0.375	1.38
Reich	5.22	.055	0.511	1.22
Aleksandrov	∞	.092	0.535	1.17

Such behavior is not always observed. The simplifying assumptions of the Bloch-Grüneisen model are:

1. Elastic scattering of the electrons by the phonons is assumed.
2. A Debye spectrum is assumed for the phonons.
3. The microscopic scattering cross-section for the electron-phonon interaction is assumed to be independent of the scattering angle. (The relaxation time is assumed isotropic.)
4. Umklapp (U) processes in which a reciprocal lattice vector is included in momentum conservation are not included.

With these approximations, it is surprising that the resistivity of a real metal would even approximate the T^5 law.

Pytte (37), Kaveh and Wiser (38), and Klemens and Jackson (15) have shown that consideration of U processes alters the phonon resistivity considerably. In calculating the resistivity of aluminum, Pytte (37) has shown that when U process are included, a T^4 term appears, and for temperatures below the cutoff for U processes, the resistivity falls off more rapidly than T^4. Kaveh and Wiser (38) calculated the resistivity for sodium, and having taken account of U processes and the momentum dependence of the electron-phonon scattering amplitude they accounted for the observed change from $T^5 (T > 9°K)$ to $T^6 (T < 9°K)$ in the temperature dependence of the resistivity. They assert further that the T^5 behavior of the resistivity of a metal has nothing to do with the Bloch result, but is merely a fortuitous numerical accident. The theory of Klemens and Jackson (15) predicts the U processes will not affect the temperature dependence, but will enhance the coefficient of the T^5 term. In considering the effect of impurity scattering in the Klemens-Jackson model, Ehrlich (14) derived an added term proportional to T^2 as well as an additional enhancement to the coefficient of the T^5 term. Klemens and Jackson and Ehrlich assumed $\rho_{ph} \propto T^5$ in the absence of U processes.

Dugdale and Basinski (17) have pointed out that presence of deviations from the MR due to the two-band effect can also enhance the coefficient of the ρ_{ph} power law term in the limit, $\rho_o >> \rho_{ph}$.

Although there is little agreement among the above authors as to what the power, n, should be for $\rho_{ph} \propto T^n$, there is agreement on the premise that n is as large as or larger than the highest power observed in $\delta(T) = \rho(T) - \rho_o$, and that it is difficult to underestimate ρ_{ph} from the experimental data.

The resistivity due to phonon scattering in pure aluminum has been assumed to be the smaller of

$$\rho_{ph} = 1.56 \times 10^{-10} (\mu\Omega cm/°K^5) T^5, \qquad 5.2$$

the low temperature limit, or at high temperatures,

$$\rho_{ph} = \rho_{pure} - \rho_o. \qquad 5.3$$

The cross-over from use of Equation 5.2 to Equation 5.3 usually occurred at ~40°K. The T^2 term has been associated with electron-electron scattering (35, 36) but, as will be discussed later is most likely a deviation from the MR. The values for b reported by Reich (33) were rejected since his data were taken in the region $\rho_{ph} \simeq \rho_o$, which as will be seen later, is the region where additional deviations from MR are large, thus affecting the apparent coefficient of the T^5 term. Aleksandrov (35) relied on

data (34) from the region T > 50°K, the data taken in this study indicates n < 5, so the T^5 coefficient reported by Aleksandrov was considered unreliable. The b value for the sample measured in this study which had the lowest residual resistance was not used, since it was relatively small (.25 mm diameter) and size effects have been shown to exhibit temperature dependent deviations from the MR (21). The largest diameter sample (.5 mm) with the lowest residual resistivity (ρ_o = .0014 μΩ-cm) was chosen as the most reliable, thus giving the value for b quoted in Equation 5.2

The Deviations from Matthiessen's Rule in Aluminum Alloys

The deviations, Δ(T), from the MR for thirteen aluminum alloy wire samples are shown as Δ/ρ_o vs temperature in Figures 7 through 10. The Al-Mg system is represented in Figure 7, Al-Cu in Figure 8, Al-Zn in Figure 9, and Al-Ga in Figure 10.

The qualitative behavior of the deviations observed was the same in all cases. The temperature dependence is characterized by a sharp rise from zero for low temperatures (T < 40°K), a peak or saturation plateau in the region 40°K < T < 100°K followed by a region with $d\rho/dT \geq 0$ as 300°K is approached. Figure 11 shows the deviations from the MR for the same alloys as log Δ/ρ_o vs

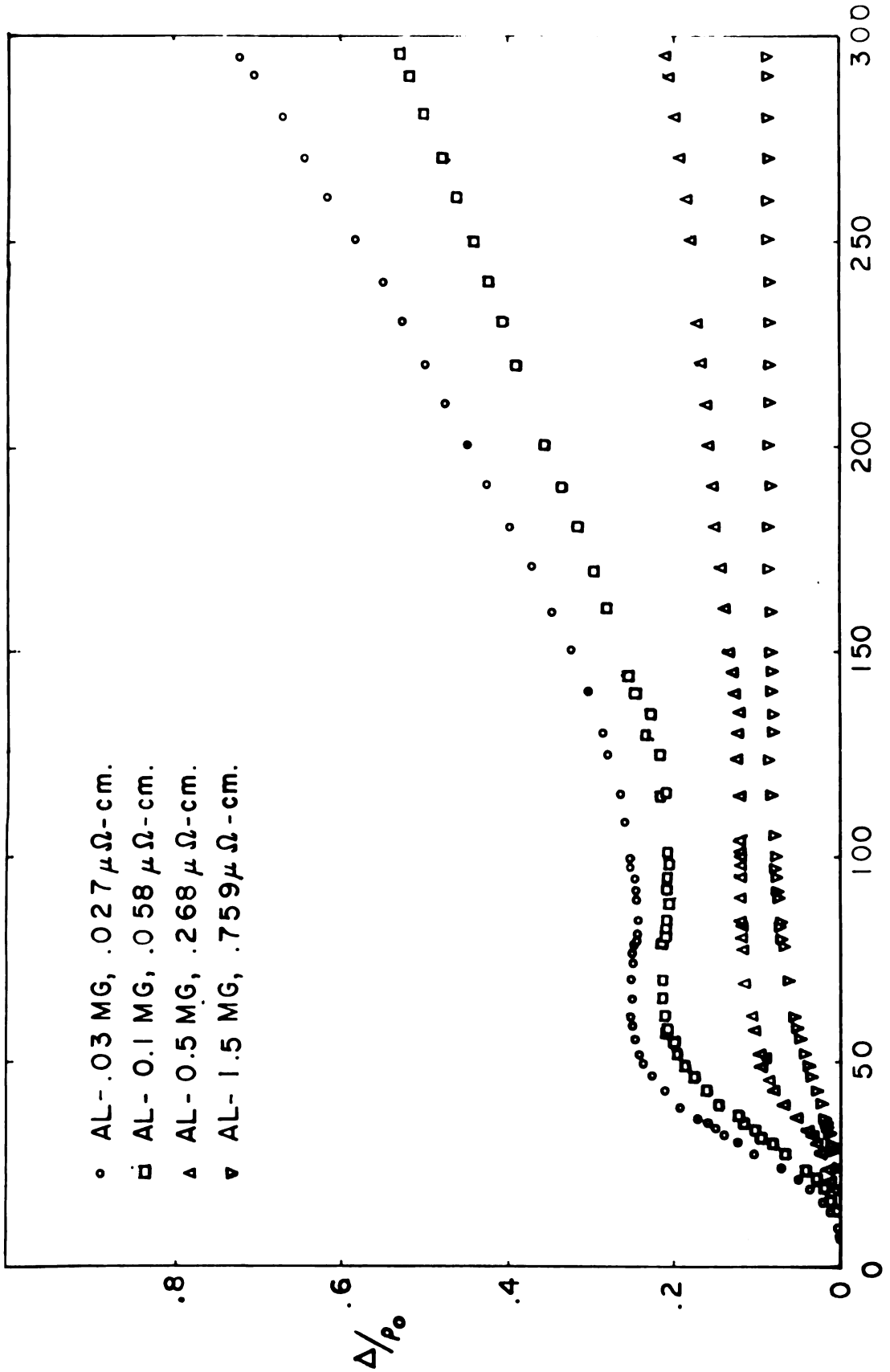

Figure 7.--Deviations from Matthiessen's Rule in Al-Mg alloys.

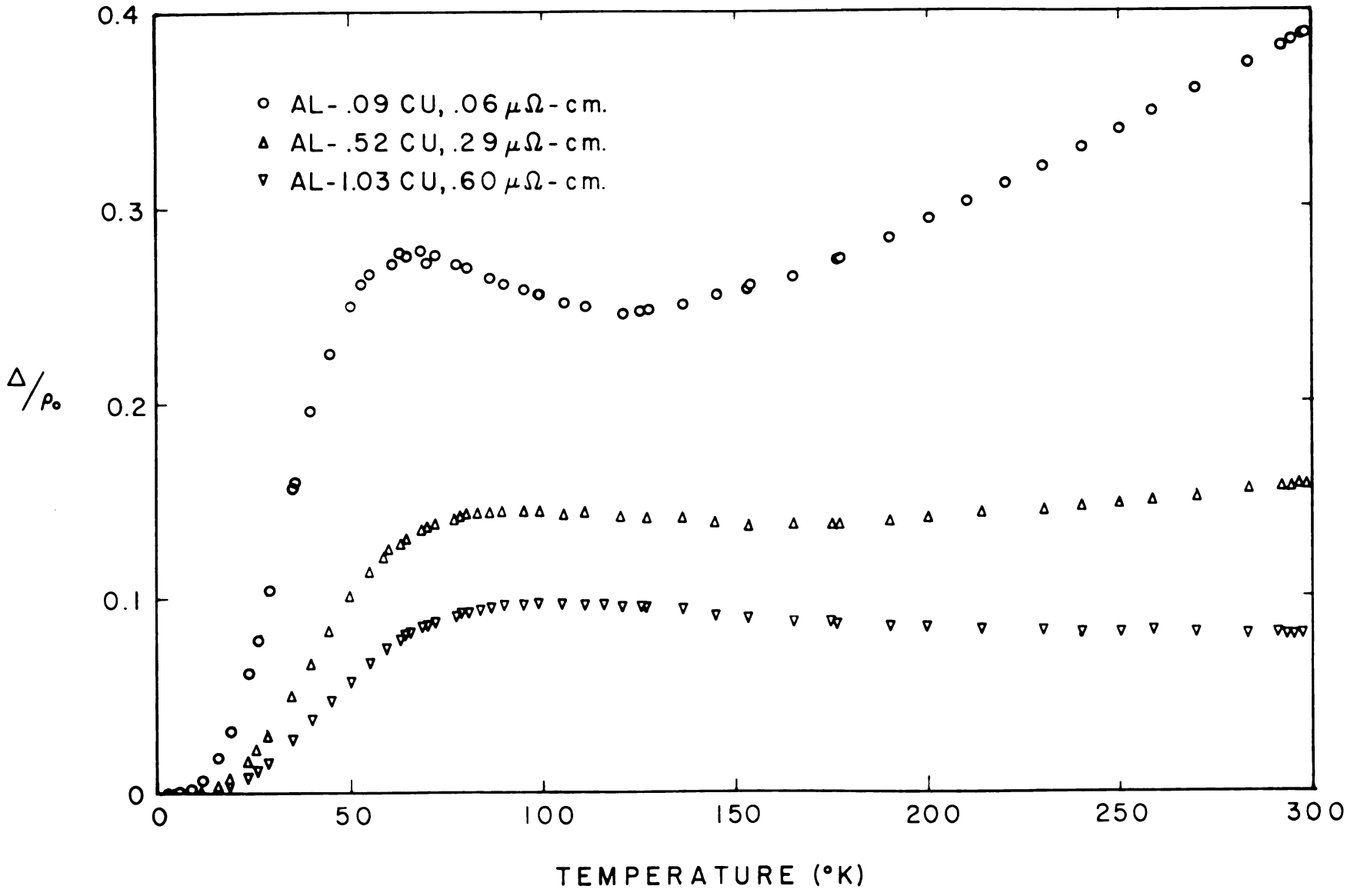

Figure 8.--Deviations from Matthiessen's Rule in Al-Cu alloys.

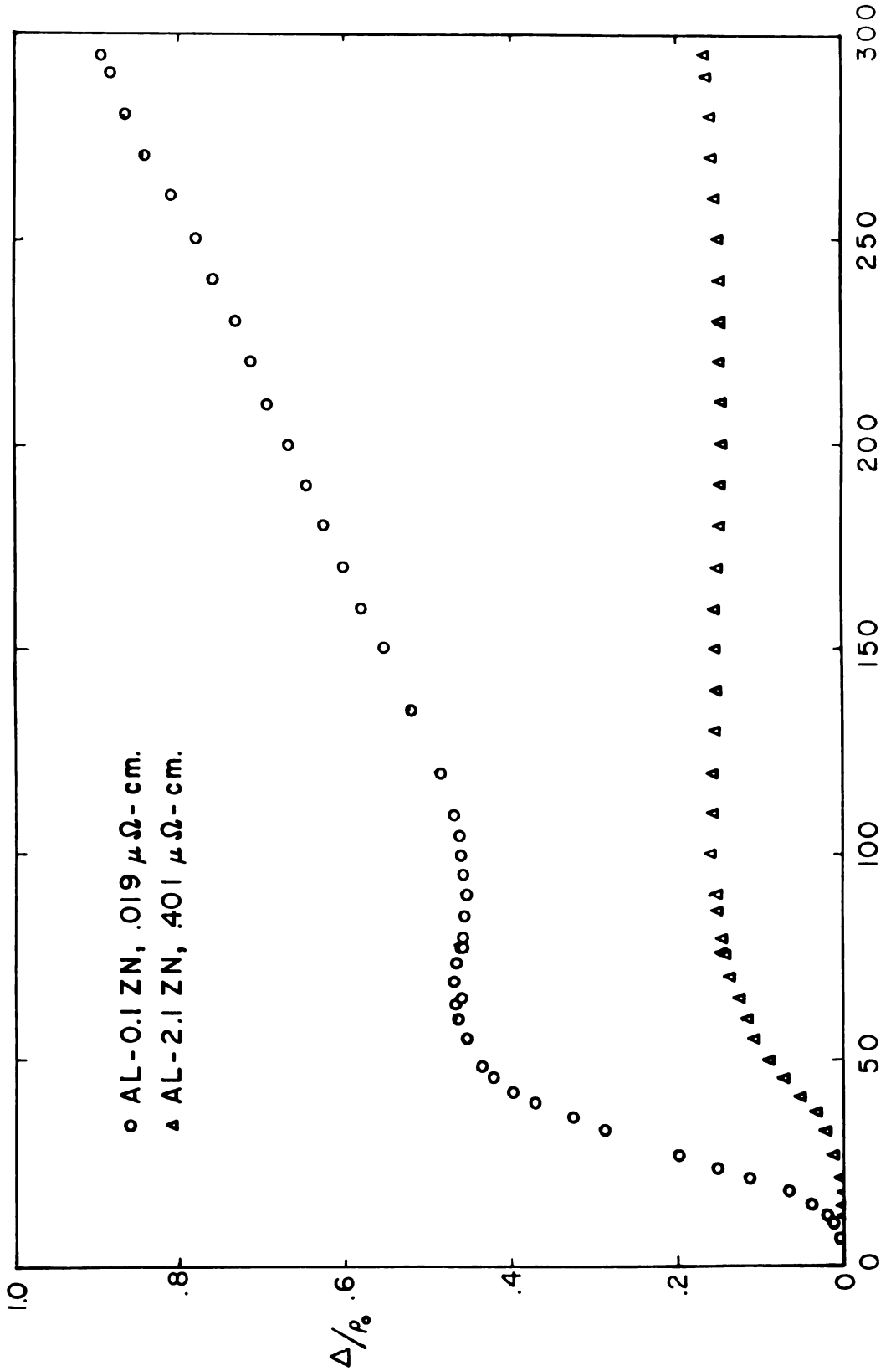

Figure 9.--Deviations from Matthiessen's Rule in Al-Zn alloys.

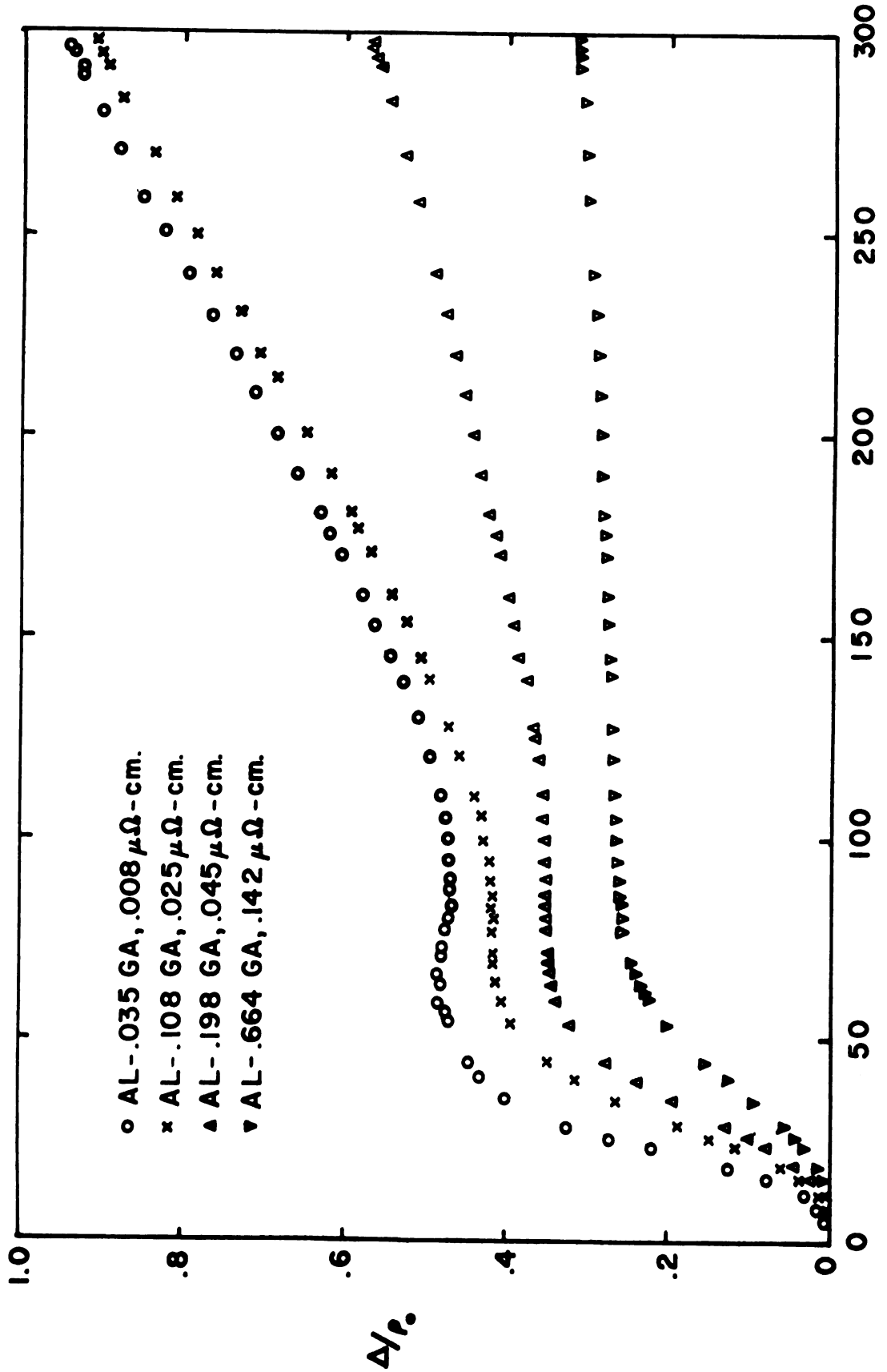

Figure 10.--Deviations from Matthiessen's Rule in Al-Ga alloys.

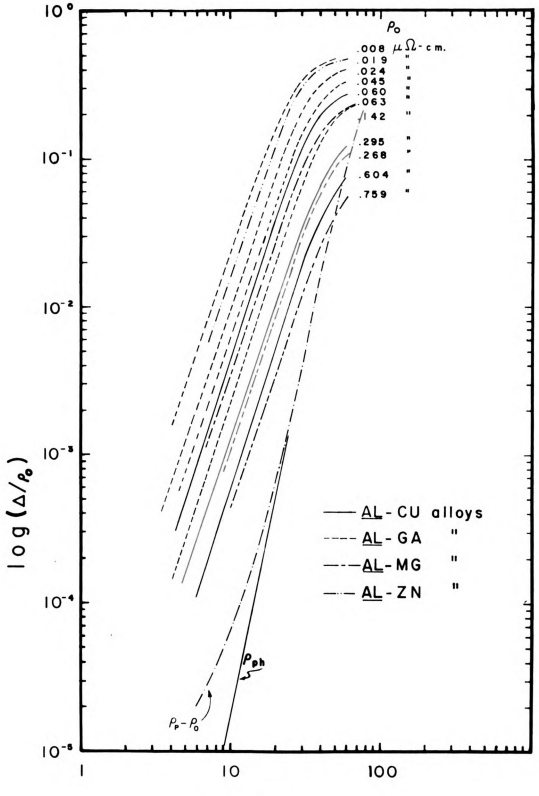

Figure 11.--Low temperature deviations from Matthiessen's Rule in aluminum alloys.

log temperature. The dominant feature of Figure 11 is that for T < 20°K

$$\Delta(T) = cT^3 \qquad 5.4$$

for all alloys.

Table 3 shows the relative corrections at 295°K due to volume change on alloying ($\delta\rho_{ph}/\rho_{ph}$) and thermal expansion ($\delta\rho_o/\rho_o$) for the most concentrated alloys of each series. The measured deviation from MR at 295°K for the 2 at/0 Zn alloy before the volume corrections was much smaller and displayed a negative temperature derivative. Thus, without volume corrections, information derived from the magnitude or temperature derivative of deviations from the MR is unreliable, particularly for the more concentrated alloys.

The residual resistivities as a function of alloy concentration for the Al-Mg, Al-Zn, Al-Ga, and Al-Cu system

TABLE 3.--Volume corrections.

Alloy	ρ_o ($\mu\Omega$-cm)	$\delta\rho_o/\rho_o$	$\delta\rho_{ph}/\rho_{ph}$	$\delta\Delta/\Delta$
Al + 1.03 Cu	.604	--	-.013	-.73
Al + .66 Ga	.142	--	.001	+.06
Al + 1.5 Mg	.759	.013	.015	+.84
Al + 2.1 Zn	.401	-.034	-.003	-.34

are shown in Figure 12. Table 4 lists the residual resistivities per atomic per cent for each of the systems.

TABLE 4.--Residual resistivity of aluminum alloys.

Alloy System	ρ_o ($\mu\Omega$-cm/atomic per cent)
Al-Mg	.52
Al-Cu	.58
Al-Zn	.19
Al-Ga	.21

From Figures 7, 8, 9, and 10, it is apparent that the deviations from the MR in the Al-Mg, Al-Cu, Al-Zn, and Al-Ga alloys are not linearly dependent on the residual resistivity, ρ_o, or in other words, the concentration. It will be shown that the data are consistent with a much weaker functional dependence. The data will be discussed in terms of the theories appropriate to such a weak functional dependence--the two-band model, the Ehrlich Theory, and the Mills Theory.

The Two-Band Model

Figure 13a shows the single OPW construction (39) of the Fermi surface of a trivalent metal such as aluminum. The pseudo-potential model of the Fermi surface, consistent with de Haas-van Alphen data, generated by the calculations of Ashcroft (40) is in topological agreement with the

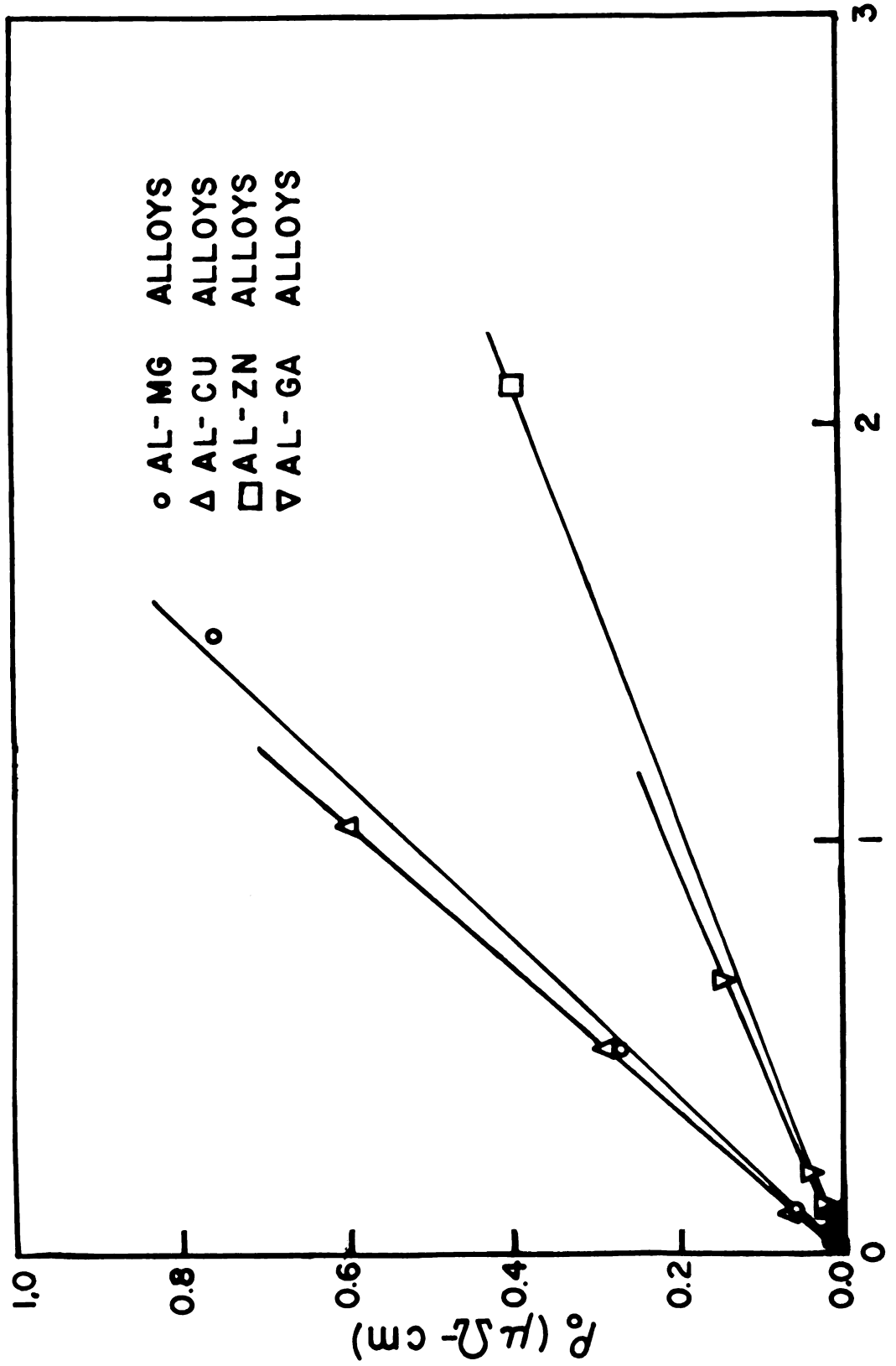

Figure 12.--Residual resistivities of aluminum alloys.

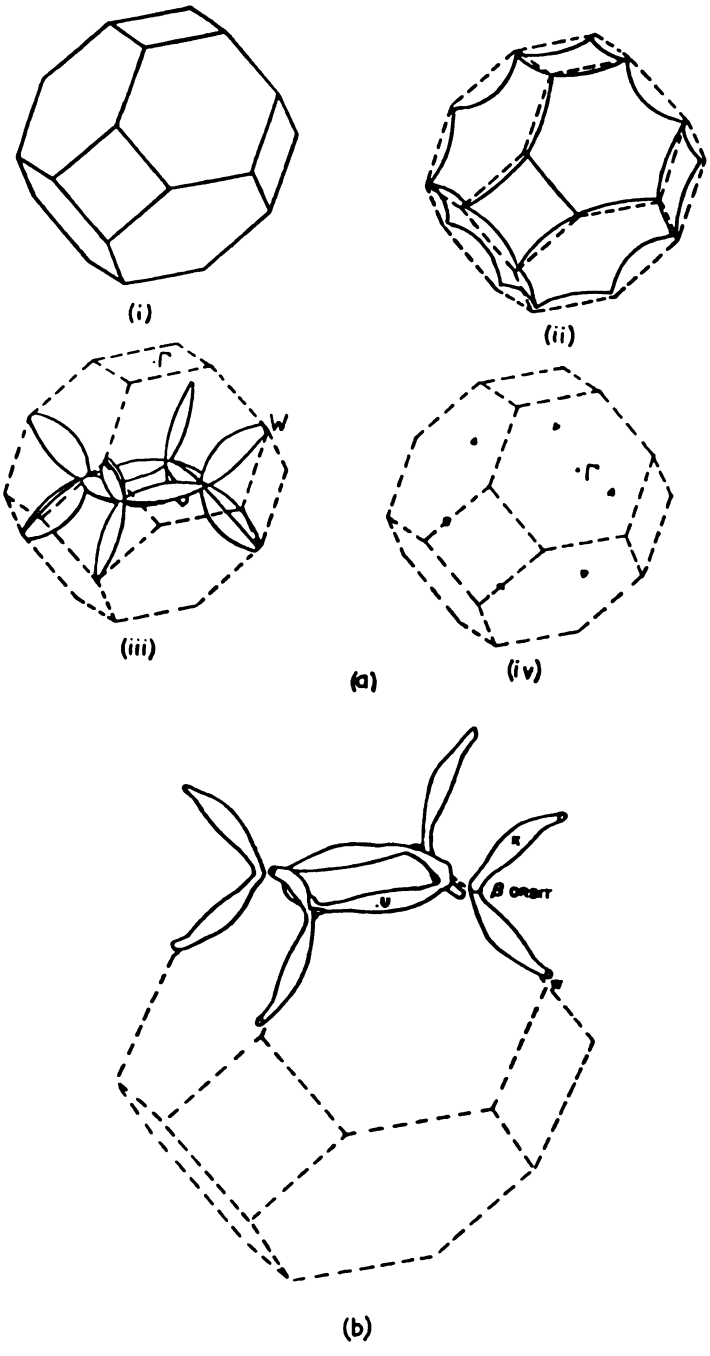

Figure 13.--Fermi surface of aluminum. (a) Single OPW construction. (b) Ashcroft model of the third Brillouin zone Fermi surface.

single OPW model. The essential features of the Ashcroft model are:

1. The first zone is full.
2. The fourth zone is empty.
3. The second zone hole surface is constructed from remapped segments of free electron spheres. The density of states is about one hole per atom and the effective mass $m^* \simeq m_e$.
4. The third zone surface is multiply connected and significantly distorted from the single OPW construction. The third zone "monster" surface is reconnected to form "rings of four" lying in the {100} planes as shown in Figure 12b. The density of states is $\simeq .02$ electron per atom and $m^* \simeq 0.1\ m_e$.

This resembles the heavy hole-light electron configuration of the semiconductor. One distinctive difference remains between the trivalent metal and the semiconductor. In contrast to the energy gap of the semiconductor, the Ashcroft model predicts 24 points of contact onto the third zone from the second zone at points identified as R by Ashcroft, lying near the symmetry point W.

The reversal of the Hall field for aluminum and aluminum alloys has been reported by Luck (25) and Forsvoll and Holwech (26). The Hall coefficient is consistent with an electron density of three electrons per

atom in the low field limit, and one hole per atom for the high field limit. The model proposed by Forsvoll and Holwech follows: The electrons on the second zone Fermi surface will behave approximately like free electrons as long as they are not undergoing Bragg reflections. The probability for Bragg reflections is small in low fields and for short mean free path, because then the electrons only travel a small part of a closed orbit on the Fermi surface between collisions. Under these conditions one would therefore expect the Hall coefficient to be close to the free electron value. In high fields most of the electrons will undergo reflections in their normal lifetime, and because the second zone Fermi surface encloses a hole region, the reflections will tend to change the sign of the overall curvature of the electron paths. The electrons will then tend to drift towards the "wrong" side of the specimen, and give rise to a positive Hall coefficient. In the high field limit, when all the electrons travel several times around the orbit, the Hall coefficient is given by the simple formula $R_H = 1/ec(n_H-n_e)$, where n_H is the number of states enclosed by the second zone surface and n_e the number of states enclosed by the third zone surface.

In light of the evidence provided by the Hall measurements it may be appropriate to treat all transport phenomena in aluminum as two-band in character.

Sondheimer and Wilson (18) have pointed out that the MR does not hold if the electrons are considered to be independently distributed in two bands in order to approximate the anisotropy of the relaxation time. The conductivities of the two bands are additive, while the phonon and impurity resistivities are separately additive in each band. Thus, denoting band number by superscripts and conductivities by σ:

$$\sigma^{tot} = \sigma^{i} + \sigma^{j}, \tag{5.5}$$

where $$\frac{1}{\sigma^{i}} = \rho^{i} = \rho^{i}_{ph} + \rho^{i}_{o}, \tag{5.6}$$

and $$\frac{1}{\sigma^{j}} = \rho^{i} = \rho^{j}_{ph} + \rho^{j}_{o}. \tag{5.7}$$

At the absolute zero of temperature,

$$\rho_{t}(0) = \rho_{o} = \frac{\rho^{i}_{o}\ \rho^{j}_{o}}{\rho^{i}_{o} + \rho^{j}_{o}} \tag{5.8}$$

and for the ideally pure metal ($\rho_{o} = 0$)

$$\rho_{ph} = \frac{\rho^{i}_{ph}\ \rho^{j}_{ph}}{\rho^{i}_{ph} + \rho^{j}_{ph}}. \tag{5.9}$$

For an alloy, the resistivity as a function of temperature is then given by

$$\rho_t = \rho(T) = \rho_{ph} + \rho_o + \frac{(\alpha-\beta)^2\rho_o\rho_{ph}}{\alpha(1+\beta)^2\rho_o + \beta(1+\alpha)^2\rho_{ph}}, \quad 5.10$$

where the last term is the apparent deviation from the MR. The parameters α and β are defined as:

$$\alpha = \frac{\rho_{ph}^i}{\rho_{ph}^j}, \text{ and } \beta = \frac{\rho_o^i}{\rho_o^j}. \quad 5.11$$

Kohler (19) obtained a similar result based on a variational solution of the collision operators for the impurity and phonon scattering. Kohler pointed out that the deviation represented in Equation 5.10 could be zero only if relaxation times could be unambiguously defined for both the phonon and impurity scattering and if their ratio is independent of electron momentum.

The expression,

$$\Delta(T) = \frac{(\alpha-\beta)^2\rho_o\rho_{ph}}{\alpha(1+\beta)^2\rho_o + \beta(1+\alpha)^2\rho_{ph}}, \quad 5.12$$

or the equivalent expression,

$$\frac{\rho_o}{\Delta} = \frac{m}{\rho_{ph}}\rho_o + b, \quad 5.13$$

where $$m = \frac{\alpha(1+\beta)^2}{(\alpha-\beta)^2} \quad 5.14$$

and $$b = \frac{\beta(1+\alpha)^2}{(\alpha-\beta)^2}, \qquad 5.15$$

are referred to as the Kohler-Sondheimer-Wilson (KSW) equations. If the deviations from the MR can be shown to fit the KSW equations, then this constitutes an element of evidence that two-band effects are responsible for the observed deviations from the MR.

The deviations from the MR in alloys of aluminum with magnesium, copper, zinc, or gallium fit the KSW equation. Figures 14, 15, and 16 show the $\Delta(T)$ data for T = 30°K, 70°K, and 295°K respectively, plotted in the form of Equation 5.13. The fit in Figure 16 is not particularly good, as the accuracy of determination of Δ may be as poor as 50 per cent. The effect of the volume corrections to the phonon and residual resistivities on the calculations of Δ is shown in Figure 16. The data reported by Seth and Woods (11) is also shown. Using the slopes and intercepts of the straight line fit for each alloy series on the KSW plot at a given temperature, the parameters α and β required for a fit to the KSW equation were calculated from 8°K to 100°K. Above 100°K, uncertainties in measurements and volume corrections did not permit unequivocal determination of α and β.

Equation 5.12 shows that $\Delta > 0$ for all $\rho_o \neq 0$. Consequently, a non-zero deviation from the MR is implicit in the phonon resistivity calculation of Equation 5.3.

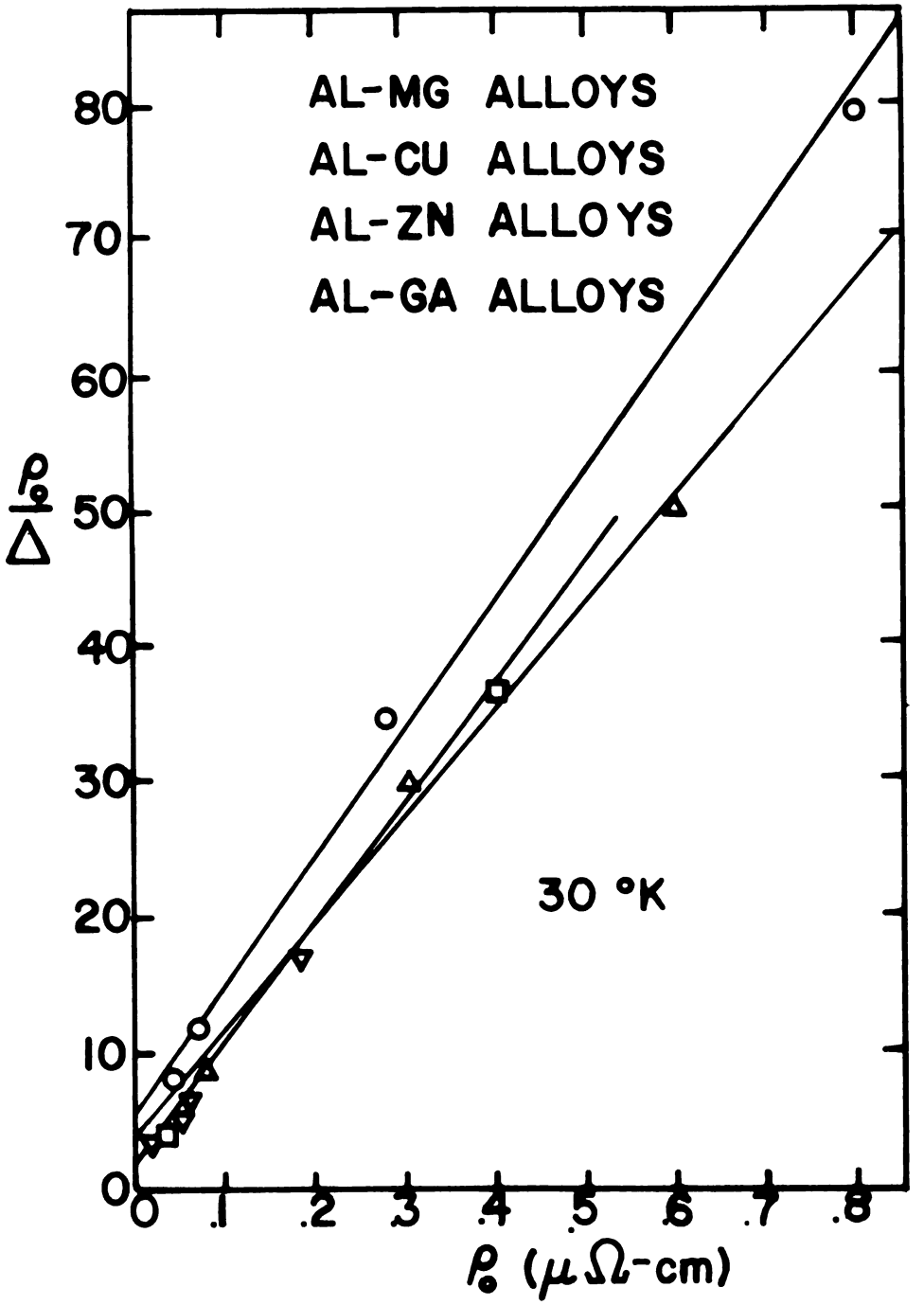

Figure 14.--Kohler-Sondheimer-Wilson plot at 30°K.

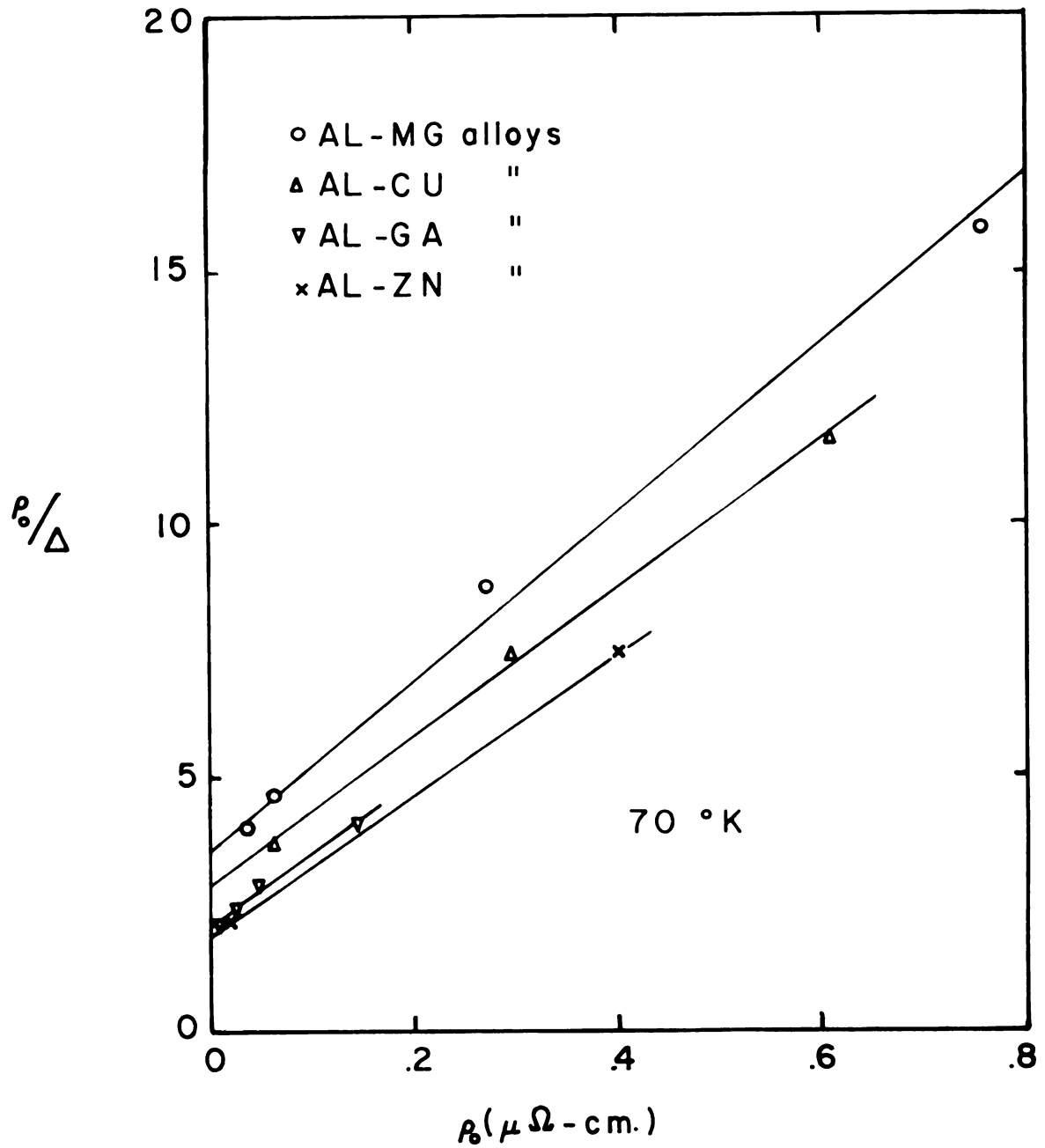

Figure 15.--Kohler-Sondheimer-Wilson plot at 70°K.

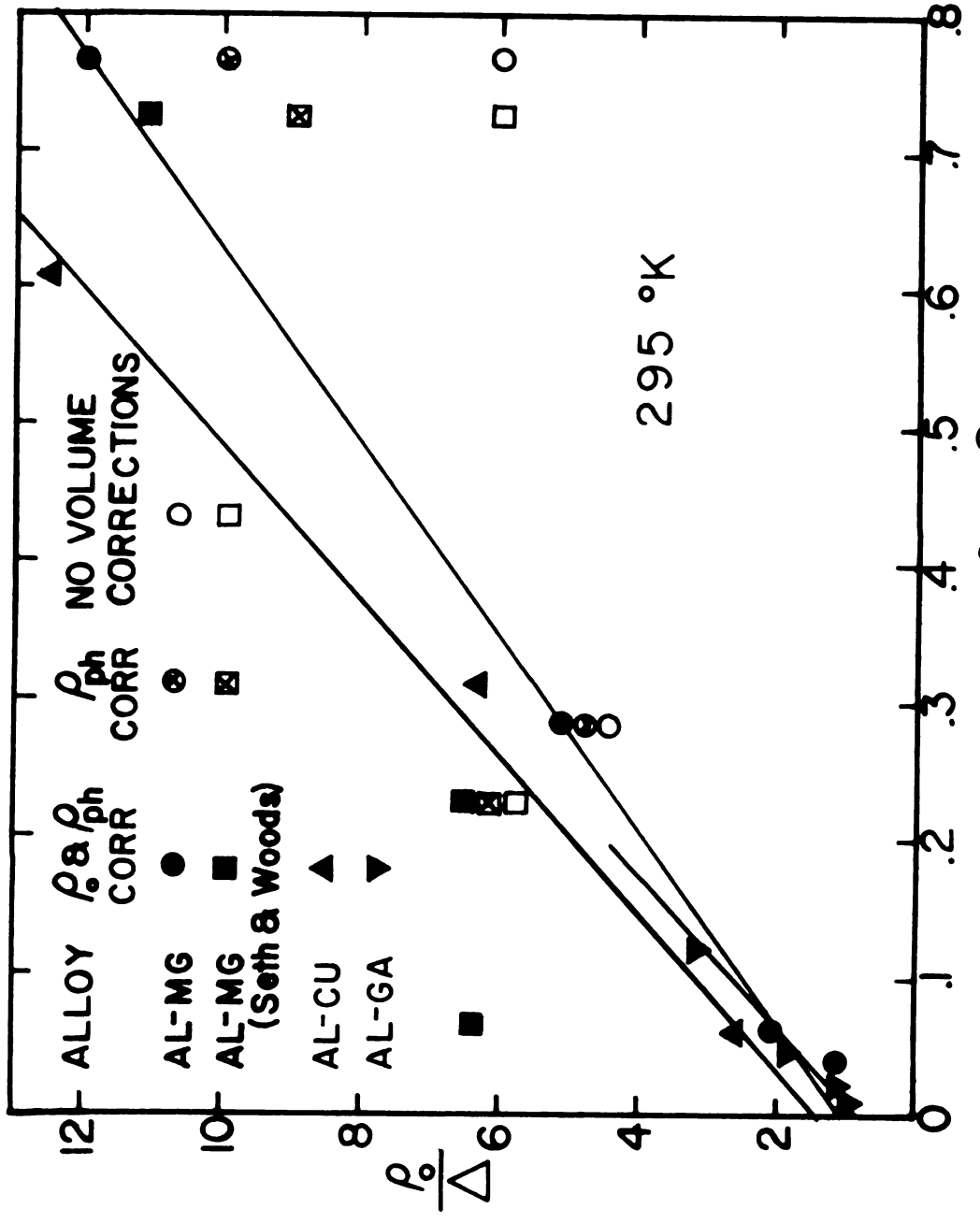

Figure 16.--Kohler-Sondheimer-Wilson plot at 295°K.

In the temperature regions for which Equation 5.3 was the appropriate definition for ρ_{ph}, corrections were made to ρ_{ph} to insure the inferred deviation from the MR in the pure sample was consistent with that observed in the alloy samples. A KSW plot was generated using the uncorrected ρ_{ph}. The average intercept

$$b = \lim_{\rho_o \to 0} \frac{\rho_o}{\Delta}, \qquad 5.16$$

was used to calculate a ρ_{ph} from the pure data consistent with the alloy data, $\rho_{ph}(T) = \rho_p(T) - \rho_o(1 + 1/b)$, which was then used to generate another KSW plot. Usually one more iteration yielded self-consistency to within the accuracy of the dimensional measurements.

The parameters α and β are shown in Figure 17. The parameter α is strongly temperature dependent varying from $\sim 10^4$ at 8°K to ~2 at 100°K, while β is relatively insensitive to change in temperature in this range. Two inconsistencies with the two-band model are apparent in Figure 17. The variation in β with temperature is not anticipated since ρ_o^i and ρ_o^j are assumed to be temperature independent. The two band approximation may not fully represent the relaxation time anisotropies, or additional mechanisms may give a temperature dependent ρ_o for one or both of the bands. The KSW scheme for extracting α and β, however, rely heavily on a constant impurity resistivity. Below 20°K the value for β is quite sensitive to the choice of

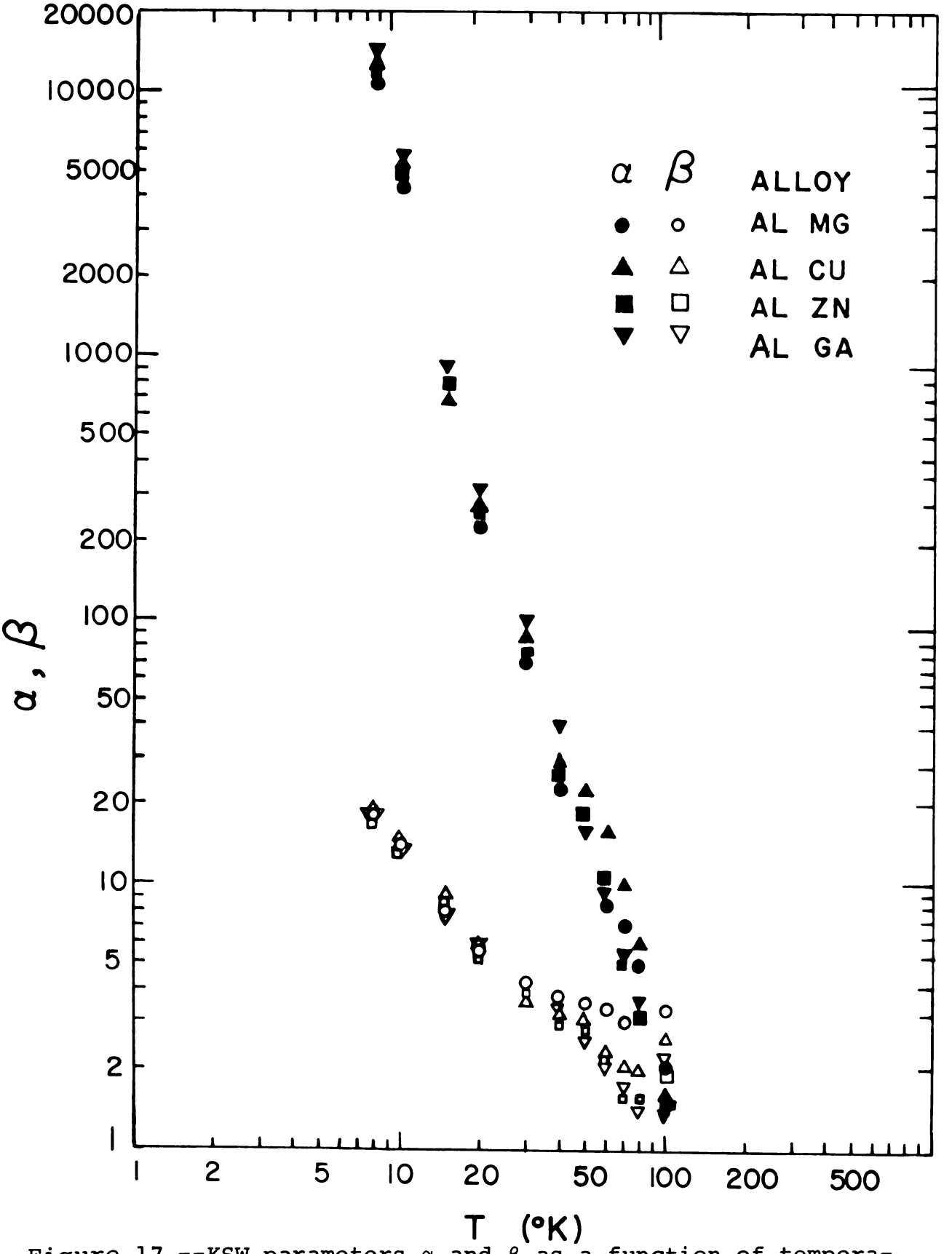

Figure 17.--KSW parameters α and β as a function of temperature.

intercept in the KSW plot, which in turn is quite sensitive to deviations in the MR implicit in Equation 5.2. If the T^5 coefficient were about 20% smaller, $\beta = 4 \pm 2$ would fit to within the precision of the experiment. A flaw of an even more serious nature is evident at about 90°K, where Figure 17 shows $\alpha = \beta$. This would be consistent with the two-band model only if deviations from Matthiessen's rule were zero at the temperature for which $\alpha = \beta$. This is the region where thermal expansion begins to be important, and the error bars implicit make a choice of $\alpha > \beta$ possible up to 300°K.

Figure 18 shows $\rho_{ph}^{j} = (\alpha+1)\rho_{ph}/\alpha$ as a function of T, showing that for $T \leq 60°K$, ρ_{ph}^{j} is of the form bT^5. The total phonon resistivity ρ_{ph} follows the same power law for $T < 40°K$, but follows a weaker temperature dependence at higher temperatures. The error bars shown indicate the magnitude of the uncertainties for the points representing ρ_{ph} and ρ_{ph}^{j}. Below 30°K, $\alpha >> 1$ and ρ_{ph}^{j} cannot be distinguished from ρ_{ph}. In contrast to ρ_{ph}^{j}, $\rho_{ph}^{i}(T) = (\alpha+1)\rho_{ph}$ is linear in T as shown in Figure 19. Below 20K the indeterminant nature of α makes the calculated values for ρ_{ph}^{i} quite uncertain. Using the evidence summarized in Figures 18 and 19, it is proposed that the bands i and j represent the states on the third zone electron and second zone hole surfaces of the aluminum Fermi surface, respectively.

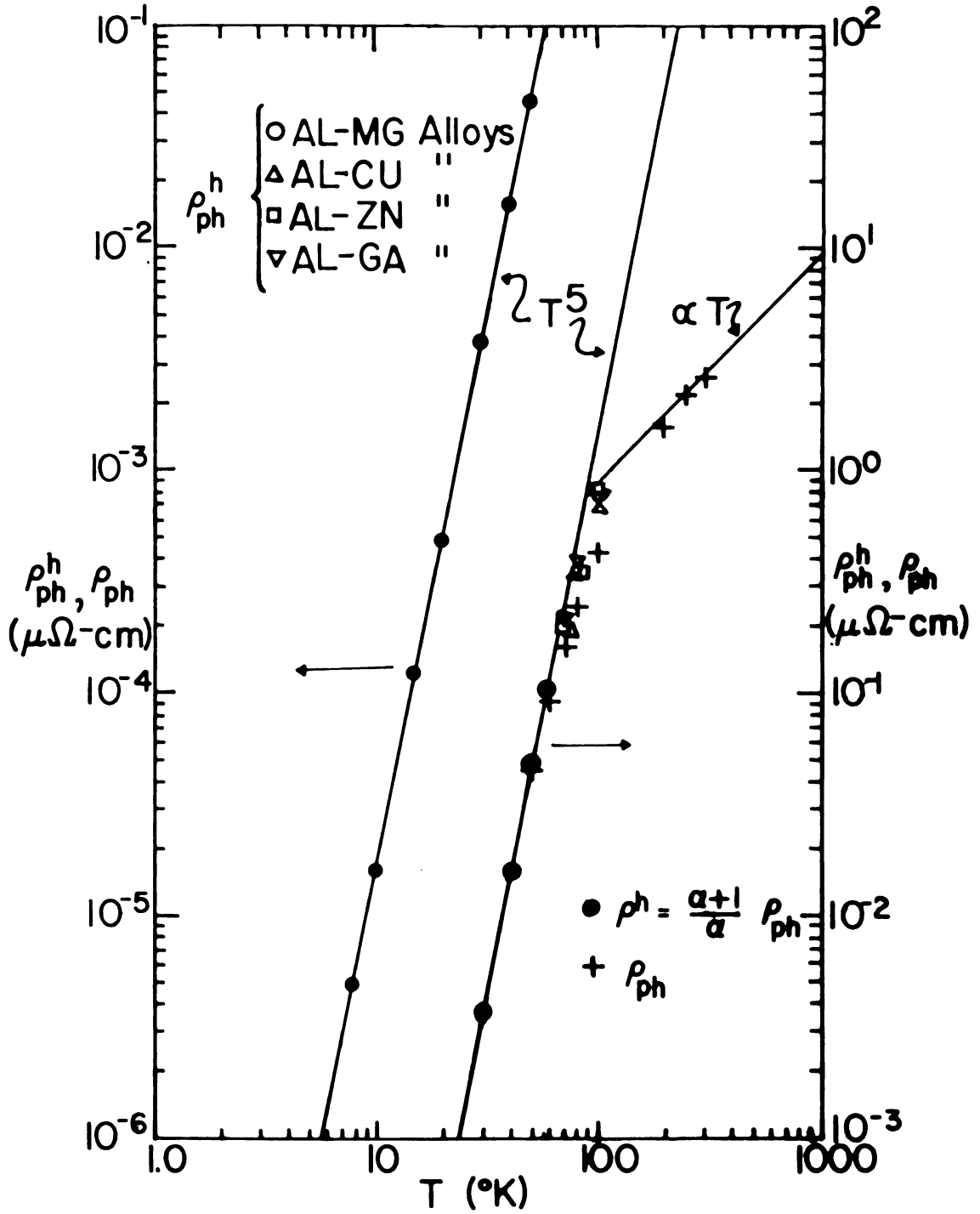

Figure 18.--Phonon resistivity of the hole band.

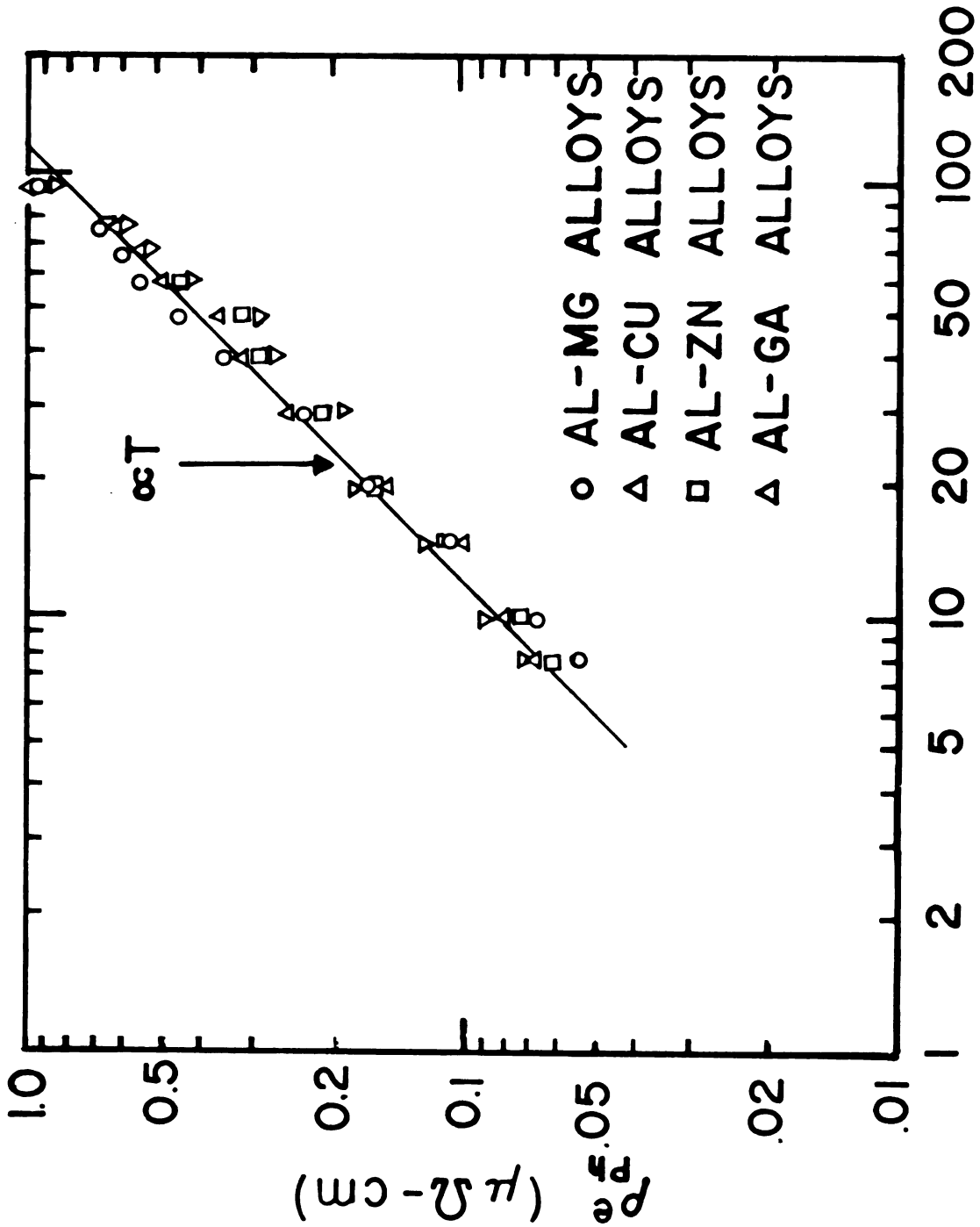

Figure 19.--Phonon resistivity of the electron band.

Phonon resistivity linear in temperature is usually associated with segments of the Fermi surface with dimensions such that the phonon wave vector, $\vec{q}_b$, necessary for large electron wave vector scattering angles has a population density, $n(\vec{q}_b) \gtrsim 1$. Where

$$n(\vec{q}_b) = (e^{\hbar\omega/kt}-1)^{-1}. \qquad 5.17$$

The characteristic temperature for which $n(\vec{q}_b) \simeq 1$ is defined by

$$T(\vec{q}_b) = \frac{h\omega_q}{k}, \qquad 5.18$$

where ω_q is the frequency of the phonon $\vec{q}_b$. Figure 20 shows such an event scattering an electron from the state $\vec{k}_i$ to $\vec{k}_f$ on the external cross-section of an arm of the third zone of the Ashcroft model of the aluminum Fermi surface. Hartmann (41) has fit neutron diffraction data to a dynamical model of the aluminum lattice giving the phonon dispersion shown in Figure 21. The phonons $\vec{q}_b$ ($\simeq 10^7$ cm^{-1}), which are appropriate for the scattering event shown in Figure 20 have $\omega_q \simeq 40 \times 10^{11}$ sec^{-1}. Thus

$$T(q_b) \simeq \frac{(10^{-27})\text{erg-sec}(40\times10^{11}\text{sec}^{-1})}{1.4 \times 10^{-16}\ \text{erg}\ ^\circ\text{K}^{-1}}, \qquad 5.19a$$

giving

$$T(q_b) \simeq 30\ ^\circ\text{K}. \qquad 5.19b$$

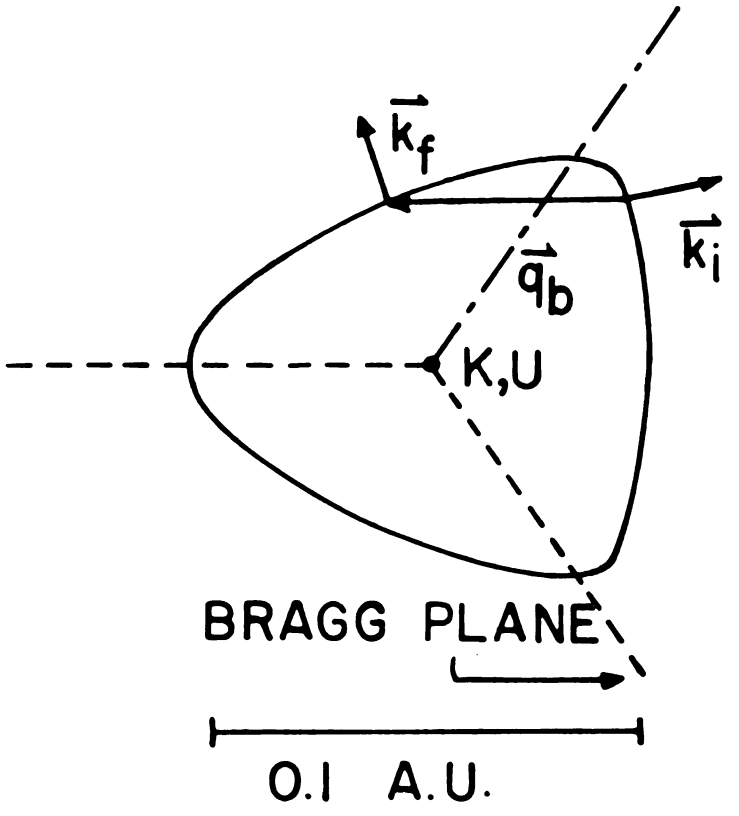

Figure 20.--Backscattering event on third zone extremal cross-section.

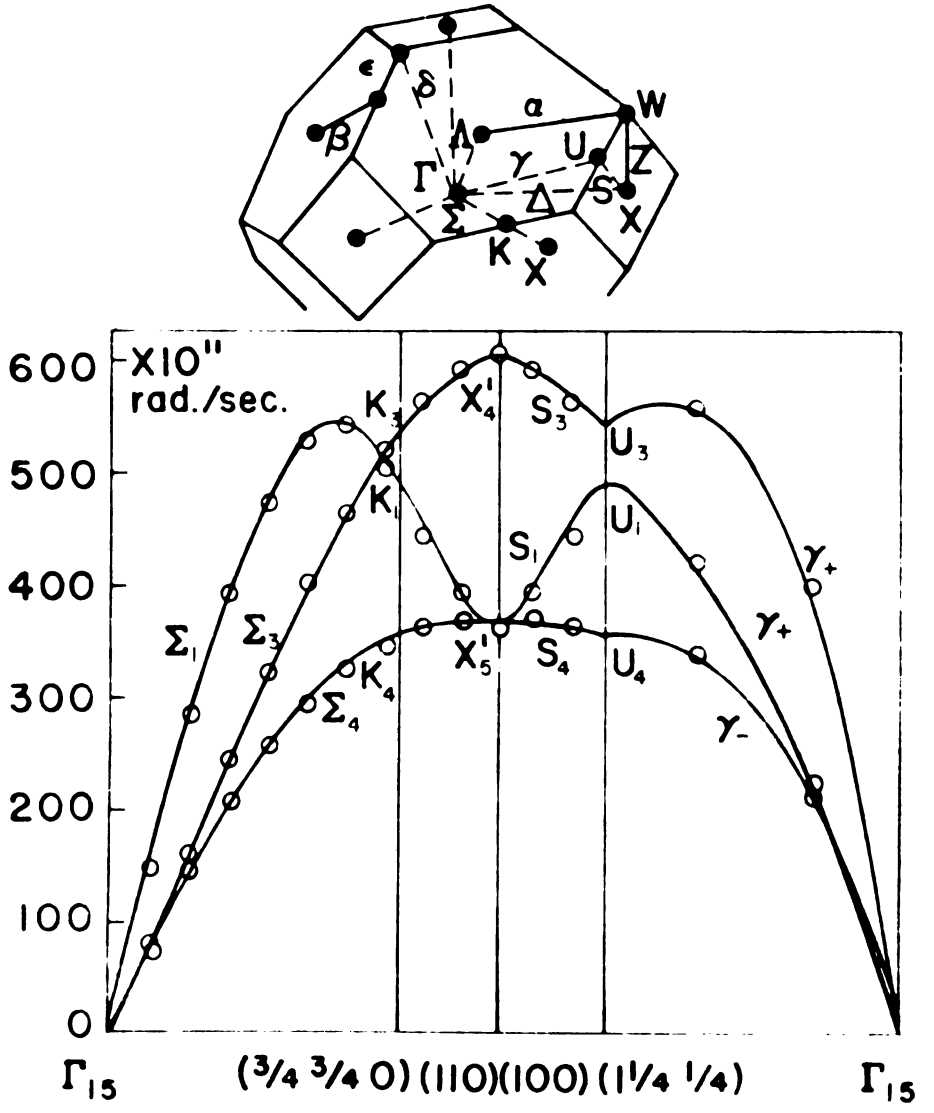

Figure 21.--Phonon dispersion spectrum for aluminum.

Since the phonon wave vector $\vec{q}_b$ crosses a Bragg plane, a reciprocal lattice vector also enters into the momentum conservation for this event. Phonons such that $q \leq q_b$ can also participate in similar backscattering events. If $T(q_b) = 30°K$ then $T(q < q_b) < 30°K$ and the population of phonons capable of resistive backscattering is large enough to expect a linear temperature dependent resistivity even below 30°K. Thus, it is reasonable to interpret the linear temperature dependence of the resistivity, ρ^i_{ph}, inferred from the KSW equations as associated with the third zone electron states. We set

$$\rho^i_{ph} = \rho^e_{ph}. \qquad 5.20$$

This leaves the interpretation of the resistivity ρ^j_{ph} as being associated with the second zone hole states. Ehrlich (14) has calculated the low temperature resistivity of monovalent metals whose Fermi surface touches or nearly touches the Brillouin zone boundaries, extending the Klemens-Jackson (15) theory to include the simultaneous presence of impurity and thermally-induced Umklapp scattering. The second zone hole sheet of the trivalent aluminum Fermi surface when considered alone and in the extended zone scheme, is analogous to the case considered by Ehrlich. The application of the Ehrlich theory to deviations from the MR in pure aluminum will be treated later. In this case, however, the resistivity, ρ^j_{ph}, does

not exhibit the T^2 component which Ehrlich predicts for the case of U processes in the presence of impurity scattering. The T^5 component is compatible with the Ehrlich theory, assuming, as does the Ehrlich-Klemens-Jackson approach, that $\rho_{ph} \propto T^5$ for no U scattering processes.

In presenting the Bloch-Grüneisen $\rho_{ph} \propto T^5$ formalism, Ziman (42) asserts that the fifth power of T, or as has been pointed out (14, 15, 37, and 38) some other high power of T, is a characteristic quantum effect in the limit of phonon momentum too small for effective large-angle resistive backscattering. Phonons capable of direct resistive backscatter on the hole surface must extend to the region of the {100} and {110} planes in reciprocal space (see Figure 21), so $350 \times 10^{11} < \omega_q^h < 600 \times 10^{11}$ rad./sec. giving $250 < T_b^h < 430$ °K. This band then, is considerably removed, in terms of available phonon momentum, from the region where single event, large-angle scattering is anticipated. We thus set

$$\rho_{ph}^j = \rho_{ph}^h. \qquad 5.21$$

Since $\alpha > 1$ at low temperatures, the phonon resistivities of the hole and electron bands are in the order $\rho_{ph}^e > \rho_{ph}^h$. Huebener (43) has applied a two-band model to the low temperature phonon drag thermopower he has observed in aluminum alloys, and concluded that $\rho_{ph}^e > \rho_{ph}^h$ is consistent with the data.

Although the data fit the KSW equations, application of the two-band model to the deviations from the MR in these aluminum alloy systems cannot be carried out without the ambiguities previously discussed. The phonon resistivities inferred for the two bands are consistent in temperature dependence with the dimensions of the third zone sheet of electron states and second zone sheet of hole states in momentum space.

The Ehrlich Theory

The parameters a and b, of the Ehrlich (14) Theory, in Equation 1.6 are related by

$$\frac{a(P,\varepsilon)}{b(P,\varepsilon)} \propto \rho_o^{3/5} \qquad 5.22$$

for ε (angle of contact of the Fermi surface with the Brillouin zone boundary) held constant. This can be shown by dimensional analysis. The quantity a/b must have dimensions (temperature)^3. Now the only variable parameter

$$P = \frac{2\rho_o}{b_o T^5}, \qquad 5.23$$

must be fixed in terms of ρ_o and b_o, where $b_o T^5$ is the phonon resistivity in the absence of U processes. Thus

$$T^3 = \left(\frac{2\rho_o}{b_o P}\right)^{3/5} \qquad 5.24$$

so

$$\frac{a}{b} \propto (\rho_o)^{3/5}. \qquad 5.25$$

Figure 22 shows log(a/b) vs log ρ_o for the data in Table 2 and one Al-Ga alloy. Slopes corresponding to $\rho_o^{3/5}$, the theoretical relationship, and $\rho_o^{2/5}$ have been drawn. Although the Ehrlich theory predicts the correct temperature behavior for deviations from the MR for relatively pure aluminum or very dilute aluminum alloys, the coefficients do not follow the predicted $\rho_o^{3/5}$ law. Further, the T^2 term could not be detected in the low temperature resistivity of the more concentrated alloys even though the T^2 term should be about as strong as the T^3 term which was observed for T < 10°K.

Although the processes which the Ehrlich Theory considers are certainly appropriate to aluminum and aluminum alloys, the data do not support the predictions of the theory.

The Mills Theory

Mills (16) has calculated the additional resistivity $\Delta(T)$ for the second order process involving scattering from an impurity and the subsequent emission or absorption of a phonon. The result is the form

$$\Delta(T) \propto \frac{\rho_o T^3}{\rho_o + \gamma(T)}, \qquad 5.26$$

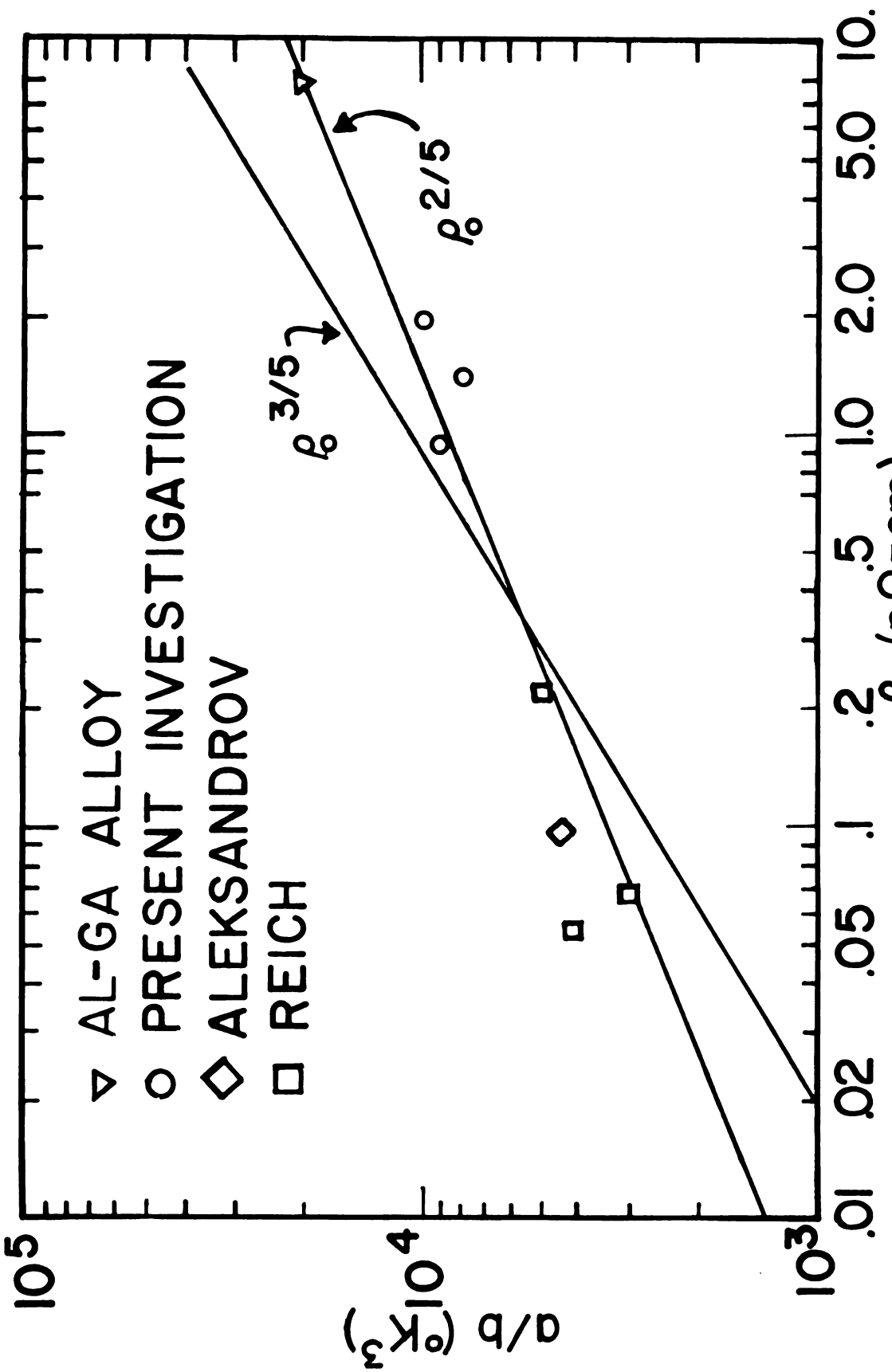

Figure 22.--Fit of the coefficients a and b to the Ehrlich Theory.

YOLLA AOS-VI
INDIASIVENI TNESERP
10²

where $\gamma(T)$ is proportional to the electron-phonon interaction relaxation rate, and $\gamma(T) \sim \rho_{ph}$. In the limit $\rho_o >> \gamma(T)$,

$$\Delta(T) = cT^3, \tag{5.27}$$

which is consistent with the data below 20°K as shown in Figure 11. The form of Equation 5.26 is also consistent with the situation that T^3 behavior is followed to higher temperatures for the more concentrated alloys. For larger ρ_o, higher temperatures must be reached before the $\gamma(T)$ term becomes important, thus altering the T^3 temperature dependence.

In order to determine the dependence of $\Delta(T)$ on the residual resistivity, $\gamma(T)$ must be included to first order. In the limit $\rho_o >> \rho_{ph} \sim \gamma(T)$:

$$\Delta(T) \propto \frac{T^3}{1 + \frac{\gamma(T)}{\rho_o}}, \tag{5.28a}$$

$$\propto T^3 \left(1 - \frac{\gamma(T)}{\rho_o}\right), \tag{5.28b}$$

$$\propto - T^3 \ln\left(\frac{\gamma(T)}{\rho_o}\right). \tag{5.28c}$$

Thus, for the T^3 region of the data,

$$\Delta(T) = cT^3 \propto T^3 \ln \rho_o - T^3 \ln T \tag{5.29}$$

so,

$$c \propto \ln \rho_o. \qquad 5.30$$

Figure 23 shows the value obtained for c from a fit of $\Delta(T)$ to Equation 5.27 as a function of log ρ_o. The dashed straight line was taken from data reported by Caplin and Rizzuto (23) for 14°K.

The points for Ekin and Maxfield (44) were taken from their published data from 1.2°K to 7°K for a monocrystalline wire (ρ_o = .85 nΩ-cm), a polycrystalline ribbon (ρ_o = .42 nΩ-cm) and a polycrystalline wire (ρ_o = .40 nΩ-cm).

At temperatures above 20°K the pure samples have a T^2 deviation from the MR. Yet, as shown in Figure 6, the T^2 deviation is replaced by some higher power of T below 20°K. Figure 11 suggests that the deviations follow a T^3 law below 15°K. The T^3 at low temperatures--T^2 at high temperatures behavior is not consistent with a simple power law composition but may be understood as the effect of the coefficient of the T^3 term modulating the temperature dependence from the T^3 low temperature limit to T^2 at higher temperatures. This is consistent with the result in Equation 5.26 if $\rho_{ph} \sim \rho_o$ and

$$\rho_o + \gamma(T) \propto T. \qquad 5.31$$

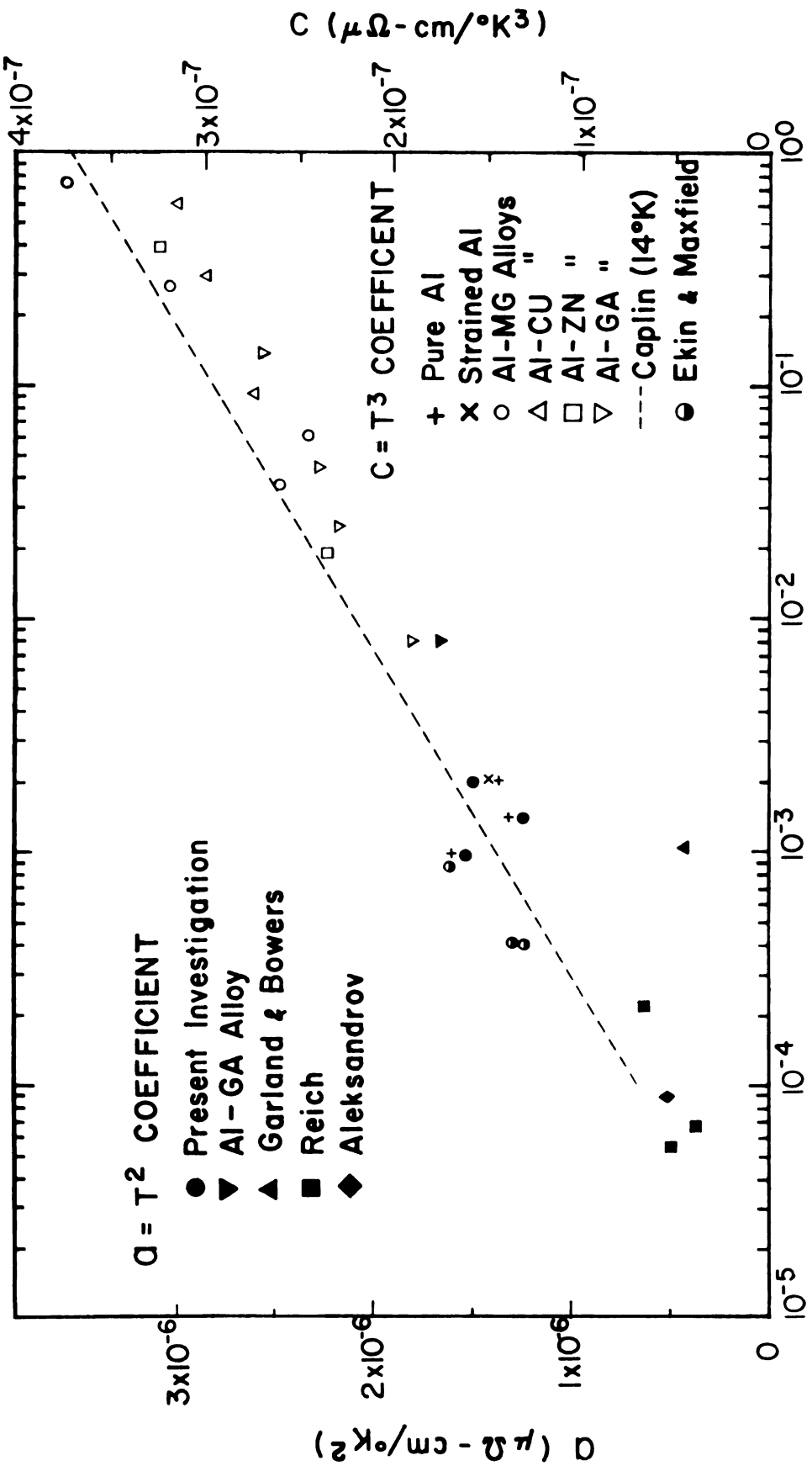

Figure 23.--Coefficients of the T^3 and T^2 terms as a function of ρ_o.

If this were the situation, one would expect the coefficients a, of the T^2 term, and b, of the T^3 term, to be proportional, and thus

$$a \propto \ln\rho_o. \qquad 5.32$$

The coefficients as listed in Table 2 and for the least dilute Al-Ga alloy are also plotted as a function of $\ln\rho_o$ in Figure 22. The change in scale was calculated from the average experimental ratio, $c/a = 0.105°K^{-1}$, for the T^3 and T^2 terms observed in the three pure samples measured in this study. The agreement in functional dependence upon ρ_o indicates that it is consistent to consider the T^2 and T^3 terms to be the intermediate and low temperature manifestations of the same effect. As pointed out in Equation 5.31, the relaxation rate must have a nearly linear temperature dependence for such a modulation effect to take place. In the pure matrix, one expects (45) that the relaxation rate $\gamma(T) \propto T^3$ for $T << \theta_D$. Consequently the assumption of Equation 5.31 is not consistent with theoretical anticipation.

The Mills Theory is successful in predicting the concentration and temperature dependence of the deviations from the MR in aluminum alloys at low temperatures. The theory is not successful at higher temperatures, since the observed temperature dependence is not consistent with that theoretically anticipated for $\gamma(T)$.

SUMMARY AND IMPLICATIONS FOR FURTHER STUDY

At low temperatures, the two-band model and the Mills Theory are both consistent with the deviations from the MR observed in the resistivity of aluminum and dilute aluminum alloys. Both theories (Equations 5.12 and 5.26) predict deviations from the MR of the form

$$\Delta(T) = \frac{\rho_o f(T)}{\rho_o + g(T)} \qquad 6.1$$

so it is necessary to weigh the relative merits of the two theories on the basis of the functions f(T) and g(T). The α and β parameters of the two-band model and the $\gamma(T)$ and T^3 terms of the Mills Theory have all shown inconsistencies between the experimentally-determined and theoretically-anticipated values.

Two-band effects have been used in considering Hall field reversals (46) in aluminum and phonon drag thermopowers of aluminum alloys (43). A coordinated effort of resistivity (and associated pressure measurements), thermopower, Hall effect, magneto resistance and thermal conductivity measurements on the same high purity aluminum and well-characterized dilute aluminum alloy samples could

provide evidence as to the relative importance of the Mills or two-band theories.

There is a further, more specific test. The Mills Theory may be construed as implying (see Figure 22) that for $\rho_o \sim 10^{-5}$ μΩ-cm, the T^2 and T^3 terms in the resistivity of aluminum should be negligible. The two-band model (Equation 5.12) predicts that for all pure samples in the region, $\rho_o >> \rho_{ph}$, the deviation from the MR is proportional to the phonon resistivity. An experimental measurement of the resistivity of pure aluminum (RR > 10^5) would be particularly useful in weighing the relative merits of the two theories.

REFERENCES

REFERENCES

1. A. Matthiessen, Ann. Physik. Chem. 110, 190(1860).

2. A. Matthiessen and C. Vogt, Ann. Physik. Chem. 122, 19(1864).

3. F. Bloch, Z. Physik 52, 555(1928).

4. F. Bloch, Z. Physik 59, 208(1930).

5. E. Grüneisen, Ann. Physik 5, 530(1933).

6. J.P.G. Shepherd and W.L. Gordon, Phys. Rev. 169, 541 (1968).

7. V.A. Bryukhanov, N.N. Delyagin and Yu. Kagan, Zh. Eksperim. i Teor. Fiz. 46, 825(1964)[Soviet Phys. JETP 19, 563(1964)].

8. V.I. Nikolaev and S.S. Yakimov, Zh. Eksperim. i Teor. Fiz. 46, 825(1964)[Soviet Phys. JETP 19, 563(1964)].

9. B. Lengler, W. Schilling, and H. Wenzl, J. Low-Temp. Phys. 2, 59(1970).

10. R.G. Stewart and R.P. Huebener, Phys. Rev. B 1, 3323 (1970).

11. R.S. Seth and S.B. Woods, Phys. Rev. B 2, 2961(1970).

12. Yu Kagan and A.P. Zhernov, Zh. Eksperim. i Teor. Fiz. 50, 1107(1966)[Soviet Phys. JETP 23, 737(1966)].

13. P.G. Klemens, J. Phys. Soc. Japan Suppl. 18, 77(1963).

14. A.C. Ehrlich, Phys. Rev. B 1, 4537(1970).

15. P.G. Klemens and J.L. Jackson, Physica 30, 2031(1964).

16. D.L. Mills, Phys. Rev. Lett. 26, 242(1971).

17. J.S. Dugdale and Z.S. Basinski, Phys. Rev. 157, 552 (1967).

18. E.H. Sondheimer and A.H. Wilson, Proc. Roy. Soc. A 190, 435(1947).

19. M. Kohler, Z. Physik 126, 495(1949).

20. P. Alley and B. Serin, Phys. Rev. 116, 334(1959).

21. J.B. Van Zytveld and J. Bass, Phys. Rev. 177, 1072 (1969).

22. G. Kh. Panova, A.P. Zhernov, and V.I. Kutaitsev, Zh. Eksperim. i Teor. Fiz. 53, 423(1967)[Soviet Phys. JETP 26, 283(1968)].

23. A.D. Caplin and C. Rizzuto, J. Phys. C: Proc. Phys. Soc., London 3, L117(1970).

24. I.A. Campbell, A.D. Caplin and C. Rizzuto, Phys. Rev. Lett. 26, 239(1971).

25. R. Lück, Phys. Stat. Sol. 18, 49(1966).

26. K. Forsvoll and I. Holwech, Phil. Mag. 10, 921(1964).

27. W.B. Pearson, A Handbook of Lattice Spacings and Structures of Metals and Alloys (Pergamon Press, Inc., New York, Vol. 1, 1958, Vol. 2, 1967).

28. P.W. Bridgman, Proc. Am. Acad. Arts Sci. 81, 169(1952).

29. G.T. Meaden, Electrical Resistance of Metals (Plenum Press, New York, 1965).

30. P.W. Bridgman, Proc. Am. Acad. Arts Sci. 84, 131(1957).

31. C.L. Foiles, private communication.

32. R.J. Corruccini and J. Gniewek, Thermal Expansion of Technical Solids at Low Temperature (U.S. Natl. Bur. Std. Monograph 29, 1961).

33. R. Reich, thesis, Université de Paris, 1965 (unpublished), cited in J.C. Garland and R. Bowers, Phys. Rev. Lett. 21, 1007(1968).

34. B.N. Aleksandrov and I.G. D'yakov, Zh. Eksperim. i Teor. Fiz. 43, 852(1962)[Soviet Phys. JETP 16, 603(1963)].

35. B.N. Aleksandrov, Dissertation, Low-temp. Physico-techn. Inst. Ukr. Acad. Sci. 1964, cited in Yu. N.

Ch'iang and V.V. Eremenko, Zh. Eksperim. i Teor. Fiz. Pis'ma v Redaktsiyu 3, 447(1966)[Soviet Phys. JETP Letters 3, 293(1966)].

36. J.C. Garland and R. Bowers, Phys. Rev. Lett. 21, 1007 (1968).

37. E. Pytte, J. Phys. Chem. Solids 28, 99(1967).

38. M. Kaveh and N. Wiser, Phys. Rev. Lett. 26, 635(1971).

39. W.A. Harrison, Phys. Rev. 118, 1190(1960).

40. N.W. Ashcroft, Phil. Mag. 8, 2055(1963).

41. W.M. Hartman (to be published, Phys. Rev. B, June 15, 1971).

42. J.M. Ziman, Electrons and Phonons (Clarendon Press, London, 1960), p. 365.

43. R.P. Huebener, Phys. Rev. 171, 634(1968).

44. J.W. Ekin and B.W. Maxfield, Phys. Rev. B 2, 4805(1970).

45. A.A. Abrikosov, L.P. Gorkov and I.E. Dzyaloshinski, Methods of Quantum Field Theory in Statistical Physics, translated and edited by R. Silverman (Prentice-Hall, Englewood Cliffs, N.J., 1963), p. 182 f.

46. N.W. Ashcroft, Phys. kondens. Materie 9, 45(1969).

APPENDICES

APPENDIX A

FORTRAN LISTING OF COMPUTER PROGRAM FOR CALCULATING RESISTIVITIES

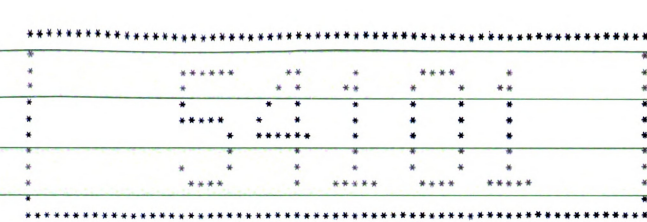

```
JOB 54101, CARTER                    00:15 MAR 22,'71      MON
LIMIT(60RE,60000),(TIME,10)
FORTRAN
      1          C   SIGMA 7 VERSION 5 OF RESCALC----ALL THERM--ALPHA--2 BAND CORR TO ROPH
      2           DIMENSION VT(100), REP(100), RES(100), TEMP(5,100), VGE(58),          00000002
      3          1TGE(58), VPT(284), TPT(284), T(100), NSAVE(5), ROS(100), ROP(100),00000003
      4          1TDELT(18), DELT(18),    AX(500), FX(500), NF(500), KP(60,101), K(5)00000004
      5          1,TP(60,101) ,TALPHA(23),ALPHA(23),ALPH(100),BETA(5,100),
      6          1 RSDELT(5,100)
      7           DIMENSION TITLE(20),VPTEP(313),TPTEP(313),DEL(100)
      8           DOUBLE PRECISION X, Y, XY, X2, DE, SM, SB
      9           DATA KM,KI,KH/1M1,1I1,1H1/                                            0000002
     10           DATA GE,PT/'GE  ','PT  '/                                             00000026
     11           DATA BLANK/'    '/                                                    00000027
     12           DATA TDELT/
     13          1 0.,2.5, 4.2, 6.0, 9.0, 11.74, 15.89, 18.86,25., 30., 40., 50.,
     14          1 60., 80., 100., 120., 200., 300./
     15           DATA DELT/
     16          1  0., .0003, .0052, .008, .045, .094, .1934,.2714, .43, .54,
     17          1 .625, .65, .62, .48, .41, .36, .46, .66/
     18           DATA TALPHA/
     19          1  0.0,  10.0,  20.0,  30.0,  40.0,  50.0,  60.0,  70.0,  80.0,
     20          190.0, 100.0, 120.0, 140.0, 160.0, 180.0, 200.0, 220.0, 240.0,
     21          1 260.0, 273.0, 280.0, 293.0, 300.0/
     22           DATA ALPHA/
     23          1 .00415, .00415, .00415, .00414, .00413, .00410, .00405, .00399,
     24          1 .00391, .00381, .00370, .00343, .00312, .00277, .00240, .00201,
     25          1 .00160, .00118, .00075, .00045, .00030, .00000, -.00016/
     26           DATA VGE/                                                             00000028
     27          112547.000, 8180.000, 5803.000, 4293.000, 3335.000, 2663.000,         000000
     28          1 2201.000, 1850.000, 1575.600, 1358.300, 1183.700, 1040.100,         00000030
```

```
     1  913.000,  816.200,  727.800,  588.500,  482.100,  399.100,      0000003
     1  333.600,  282.100,  241.100,  207.300,  180.400,  158.800,      00000032
     1  140.400,  113.140,   93.660,   79.420,   68.690,   60.400,      00000033
     1   53.890,   48.600,   44.220,   40.560,   37.450,   32.400,      00000034
     1   28.500,   25.370,   22.820,   20.690,   18.900,   17.370,      00000035
     1   16.050,   14.900,   13.900,   11.892,   10.388,    9.231,      00000036
     1    8.328,    7.606,    7.020,    6.543,    6.152,    5.823,      00000037
     1    5.545,    5.307,    5.145,    5.112/                          00000038
      DATA TGE/                                                         0000003
     1   1.50,   1.75,   2.00,   2.25,   2.50,   2.75,   3.00,   3.25,   3.50,  00000040
     1   3.75,   4.00,   4.25,   4.50,   4.75,   5.00,   5.50,   6.00,   6.50,  0000004
     1   7.00,   7.50,   8.00,   8.50,   9.00,   9.50,  10.00,  11.00,  12.00,  00000042
     1  13.00,  14.00,  15.00,  16.00,  17.00,  18.00,  19.00,  20.00,  22.00,  00000043
     1  24.00,  26.00,  28.00,  30.00,  32.00,  34.00,  36.00,  38.00,  40.00,  00000044
     1  45.00,  50.00,  55.00,  60.00,  65.00,  70.00,  75.00,  80.00,  85.00,  00000045
     1  90.00,  95.00,  99.00, 100.00/                                   00000046
      DATA VPT/                                                         00000047
     1  867.497803,  967.085938, 1072.819824, 1184.611816, 1302.347656,  000000
     1 1425.885742, 1555.057861, 1689.639941, 1829.591797, 1974.567871,  000000
     1 2124.416260, 2278.941895, 2437.942383, 2601.222900, 2768.581299,  00000050
     1 2939.826904, 3114.766846, 3293.210938, 3474.973633, 3659.866211,  000000
     1 3847.717285, 4038.345215, 4231.582031, 4427.261719, 4625.226563,  00000052
     1 4825.322813, 5027.398438, 5231.320312, 5436.949219, 5644.164063,  00000053
     1 5852.839844, 6062.863281, 6274.132813, 6486.539063, 6699.992188,  00000054
     1 6914.402344, 7129.663594, 7345.757813, 7562.554688, 7780.003906,  00000055
     1 7998.042969, 8216.665469, 8435.640625, 8655.097656, 8874.921875,  00000056
     1 9095.079313, 9315.500000, 9536.171875, 9757.046875, 9978.578125,  00000057
     1 10200.68231, 10421.73828, 10643.50391, 10865.36719, 11087.29688,  00000058
     1 11309.26953, 11531.27344, 11753.28516, 11975.23906, 12197.26953,  00000059
     1 12419.21094, 12638.98438, 12860.89063, 13082.72656, 13304.46875,  00000060
     1 13526.12109, 13747.66797, 13969.10156, 14190.41797, 14411.60938,  0000006
     1 14632.67188, 14853.50375, 15074.37891, 15295.01953, 15515.51172,  00000062
     1 15736.85547, 15956.03906, 16176.07031, 16395.94531, 16615.66016,  00000063
     1 16835.21094, 17054.60547, 17273.83203, 17492.89453, 17711.79688,  00000064
     1 17930.53125, 18149.10547, 18367.51172, 18585.75781, 18803.83984,  00000065
     1 19021.75781, 19239.51563, 19457.10938, 19674.54688, 19891.82031,  00000066
     1 20108.94141, 20325.90234, 20542.71094, 20759.36328, 20975.86328,  00000067
     1 21192.21094, 21408.41016, 21624.45703, 21840.35938, 22056.11719,  0000006
     1 22271.72656, 22487.20313, 22702.53125, 22917.71875, 23132.76953,  00000069
     1 23347.68359, 23562.46094, 23777.10547, 23991.61719, 24206.00391,  00000070
     1 24420.25781, 24634.38281, 24848.33281, 25062.25781, 25276.00781,  00000071
     1 25489.64063, 25703.14453, 25916.53516, 26129.80469, 26342.95703,  00000072
     1 26556.00000, 26768.92578, 26981.73828, 27194.43750, 27407.02734,  00000073
```

```
      127619.507812,27831.878906,28044.148437,28256.304687,28468.355469,  00000074
      128680.306594,28892.160156,29103.902344,29315.546875,29527.093750,  00000075
      129738.535156,29949.886719,30161.132812,30372.292969,30583.351562,  00000076
      130794.316406,31005.187500,31215.964844,31426.648437,31637.242187,  00000077
      131847.746094,32058.132812,32268.460937,32478.636719,32688.808594,  0000007
      132898.894531,33108.855469,33318.722656,33528.531250,33738.281250,  00000079
      133947.875000,34157.406250,34366.878906,34576.292969,34785.582031,  00000080
      134994.781250,35203.917969,35412.992187,35621.945312,35830.871094,  00000081
      136039.703125,36248.410156,36457.058594,36665.679687,36874.144531,  00000082
      137082.609375,37290.890625,37499.234375,37707.394531,37915.527344,  00000083
      138123.562500,38331.511719,38539.457031,38747.250000,38954.953125,  00000084
      139162.687500,39370.269531,39577.816406,39785.246094,39992.644531,  00000085
      140199.980469,40407.164062,40614.347656,40821.441406,41028.500000,  00000086
      141235.472656,41442.320312,41649.136719,41855.894531,42062.589844,  00000087
      142269.199312,42475.707031,42682.187500,42888.578125,43094.906250,  000000 8
      143301.175781,43507.414062,43713.531250,43919.585937,44125.609375,  00000089
      144331.511719,44537.382812,44743.222656,44948.910156,45154.601562,  00000090
      145360.226563,45565.761719,45771.207031,45976.621094,46181.972656,  000000 1
      146387.234375,46592.464844,46797.636719,47002.683594,47207.761719,  00000092
      147412.718750,47617.556781,47822.417969,48027.218750,48231.902344,  000000 3
      148436.556781,48641.140625,48845.609375,49050.109375,49254.484375,  00000094
      149458.882125,49663.085937,49867.308594,50071.441406,50275.480469,  000000 5
      150479.492187,50683.466875,50887.359375,51091.152344,51294.921875,  00000096
      151498.593750,51702.238281,51905.761719,52109.312500,52312.710937,  00000097 80
      152516.050781,52719.417969,52922.636719,53125.820312,53328.976562,  00000098
      153532.042969,53735.015625,53937.957031,54140.804687,54343.625000,  00000099
      154546.414062,54749.050781,54951.718750,55154.265625,55356.777344,  00000100
      155559.203125,55761.625000,55963.894531,56166.136719,56368.375000,  00000101
      156570.492188,56772.582031,56974.609375,57176.511719,57378.417969,  00000102
      157580.257812,57782.042969,57983.703125,58185.363281,58386.929687,  00000103
      158588.437500,58789.832812,58991.332031,59192.656250/               00000104
       DATA                                                 IPI/30.0, 31.0, 32.0,  00000106
     1 33.0, 34.0, 35.0, 36.0, 37.0, 38.0, 39.0, 40.0, 41.0, 42.0,        00000107
     1 43.0, 44.0, 45.0, 46.0, 47.0, 48.0, 49.0, 50.0, 51.0, 52.0,        00000108
     1 53.0, 54.0, 55.0, 56.0, 57.0, 58.0, 59.0, 60.0, 61.0, 62.0,        0000010
     1 63.0, 64.0, 65.0, 66.0, 67.0, 68.0, 69.0, 70.0, 71.0, 72.0,        00000110
     1 73.0, 74.0, 75.0, 76.0, 77.0, 78.0, 79.0, 80.0, 81.0, 82.0,        00000111
     1 83.0, 84.0, 85.0, 86.0, 87.0, 88.0, 89.0, 90.0, 91.0, 92.0,        00000112
     1 93.0, 94.0, 95.0, 96.0, 97.0, 98.0, 99.0,100.0,101.0,102.0,        00000113
     1103.0,104.0,105.0,106.0,107.0,108.0,109.0,110.0,111.0,112.0,        00000114
     1113.0,114.0,115.0,116.0,117.0,118.0,119.0,120.0,121.0,122.0,        00000 15
     1123.0,124.0,125.0,126.0,127.0,128.0,129.0,130.0,131.0,132.0,        00000116
     1133.0,134.0,135.0,136.0,137.0,138.0,139.0,140.0,141.0,142.0,        00000117
```

```
1143.0,144.0,145.0,146.0,147.0,148.0,149.0,150.0,151.0,152.0,    00000118
1153.0,154.0,155.0,156.0,157.0,158.0,159.0,160.0,161.0,162.0,    00000119
1163.0,164.0,165.0,166.0,167.0,168.0,169.0,170.0,171.0,172.0,    00000120
1173.0,174.0,175.0,176.0,177.0,178.0,179.0,180.0,181.0,182.0,    00000121
1183.0,184.0,185.0,186.0,187.0,188.0,189.0,190.0,191.0,192.0,    00000122
1193.0,194.0,195.0,196.0,197.0,198.0,199.0,200.0,201.0,202.0,    00000123
1203.0,204.0,205.0,206.0,207.0,208.0,209.0,210.0,211.0,212.0,    00000124
1213.0,214.0,215.0,216.0,217.0,218.0,219.0,220.0,221.0,222.0,    00000
1223.0,224.0,225.0,226.0,227.0,228.0,229.0,230.0,231.0,232.0,    00000126
1233.0,234.0,235.0,236.0,237.0,238.0,239.0,240.0,241.0,242.0,    00000127
1243.0,244.0,245.0,246.0,247.0,248.0,249.0,250.0,251.0,252.0,    00000128
1253.0,254.0,255.0,256.0,257.0,258.0,259.0,260.0,261.0,262.0,    00000129
1263.0,264.0,265.0,266.0,267.0,268.0,269.0,270.0,271.0,272.0,    00000130
1273.0,274.0,275.0,276.0,277.0,278.0,279.0,280.0,281.0,282.0,    00000131
1283.0,284.0,285.0,286.0,287.0,288.0,289.0,290.0,291.0,292.0,    00000132
1293.0,294.0,295.0,296.0,297.0,298.0,299.0,300.0,301.0,302.0,    00000133
1303.0,304.0,305.0,306.0,307.0,308.0,309.0,310.0,311.0,312.0,    00000134
1313.0/                                                          00000135
 DATA VPTEP/
1  25.49,   26.31,   27.34,   28.70,   30.49,   32.66,   35.55,
1  39.31,   44.46,   51.40,   60.58,   72.23,   87.10,  104.96,
1  126.75,  152.96,  183.31,  218.17,  257.99,  302.63,  353.45,
1  409.24,  470.52,  537.93,  611.58,  692.13,  780.12,  875.23,
1  977.67, 1082.86, 1192.79, 1309.85, 1434.49, 1564.87, 1701.18,
1 1842.17, 1987.25, 2134.23, 2286.46, 2444.31, 2607.32, 2773.91,
1 2944.67, 3119.36, 3298.26, 3480.60, 3666.38, 3854.63, 4044.85,
1 4237.02, 4431.49, 4627.71, 4826.01, 5025.95, 5228.83, 5434.66,
1 5642.61, 5852.53, 6064.02, 6275.96, 6488.71, 6701.47, 6914.68,
1 7128.84, 7344.11, 7560.67, 7778.60, 7997.65, 8217.32, 8436.86,
1 8656.39, 8876.34, 9095.50, 9313.04, 9528.11, 9738.92, 9950.19,
1 10168.25, 10393.61, 10620.70, 10838.43, 11048.90, 11262.73, 11480.03,
1 11705.09, 11940.51, 12181.45, 12418.48, 12642.82, 12860.74, 13081.73,
1 13303.51, 13525.22, 13746.73, 13967.99, 14188.95, 14409.64, 14630.06,
1 14855.26, 15070.38, 15290.43, 15510.38, 15730.22, 15949.99, 16169.72,
1 16389.44, 16609.11, 16828.58, 17047.77, 17266.68, 17485.33, 17703.62,
1 17921.56, 18139.24, 18356.63, 18573.83, 18791.03, 19008.42, 19226.19,
1 19444.30, 19662.31, 19879.86, 20096.67, 20308.52, 20521.42, 20742.72,
1 20977.22, 21234.83, 21563.24, 21767.19, 22013.24, 22229.82, 22419.07,
1 22588.59, 22754.45, 22935.32, 23128.06, 23331.08, 23542.78, 23760.03,
1 23977.78, 24194.05, 24411.22, 24629.52, 24847.51, 25063.98, 25278.36,
1 25549.57, 25760.83, 25910.26, 26120.17, 26331.61, 26544.00, 26757.21,
1 26970.93, 27184.59, 27397.50, 27610.36, 27825.72, 28042.21, 28260.54,
1 28480.53, 28701.64, 28923.06, 29143.90, 29364.73, 29586.84, 29808.87,
```

```
     130028.04,30242.50,30451.41,30654.87,30853.99,31050.81,31248.27,
     131445.73,31643.97,31844.12,32046.79,32252.19,32460.01,32669.50,
     132879.45,33088.55,33297.63,33506.69,33715.78,33924.93,34134.17,
     134343.51,34552.93,34762.41,34971.91,35181.38,35390.88,35600.36,
     135809.77,36019.09,36228.31,36437.43,36646.48,36855.50,37064.56,
     137273.61,37482.80,37692.06,37900.98,38109.27,38316.77,38523.48,
     138729.53,38935.18,39140.85,39346.49,39552.18,39758.28,39965.03,
     140172.55,40380.50,40588.63,40798.75,41007.74,41216.64,41425.81,
     141634.93,41843.45,42051.05,42257.57,42463.04,42667.70,42871.95,
     143076.38,43280.94,43485.39,43689.89,43894.61,44099.65,44305.07,
     144510.84,44715.27,44923.02,45129.08,45335.26,45541.37,45747.18,
     145952.57,46157.49,46361.95,46566.09,46770.08,46974.21,47178.13,
     147381.94,47586.35,47791.83,47998.60,48206.68,48415.85,48625.65,
     148835.39,49044.87,49254.38,49464.86,49674.63,49882.48,50087.72,
     150289.10,50489.90,50687.84,50885.15,51083.38,51281.37,51479.68,
     151678.73,51878.73,52079.73,52281.63,52484.11,52686.72,52889.03,
     153091.34,53293.66,53495.97,53698.28,53900.60,54102.91,54305.22,
     154507.53,54709.85,54912.16,55114.47,55316.82,55519.19,55721.4 ,
     155923.56,56125.45,56327.12,56528.60,56729.99,56931.38,57132.81,
     157334.24,57535.67,57737.11,57938.54,58139.97,58341.40,58542.84,
     158744.27,58945.70,59147.13,59348.57,59550.00/
      DATA IPTFD/
     1  3.0,  4.0,  5.0,  6.0,  7.0,  8.0,  9.0, 10.0, 11.0, 12.0,
     1 13.0, 14.0, 15.0, 16.0, 17.0, 18.0, 19.0, 20.0, 21.0, 22.0,
     1 23.0, 24.0, 25.0, 26.0, 27.0, 28.0, 29.0, 30.0, 31.0, 32.0,
     1 33.0, 34.0, 35.0, 36.0, 37.0, 38.0, 39.0, 40.0, 41.0, 42.0,  00000107
     1 43.0, 44.0, 45.0, 46.0, 47.0, 48.0, 49.0, 50.0, 51.0, 52.0,  00000108
     1 53.0, 54.0, 55.0, 56.0, 57.0, 58.0, 59.0, 60.0, 61.0, 62.0,  00000109
     1 63.0, 64.0, 65.0, 66.0, 67.0, 68.0, 69.0, 70.0, 71.0, 72.0,  00000110
     1 73.0, 74.0, 75.0, 76.0, 77.0, 78.0, 79.0, 80.0, 81.0, 82.0,  00000111
     1 83.0, 84.0, 85.0, 86.0, 87.0, 88.0, 89.0, 90.0, 91.0, 92.0,  00000112
     1 93.0, 94.0, 95.0, 96.0, 97.0, 98.0, 99.0,100.0,101.0,102.0,  00000113
     1103.0,104.0,105.0,106.0,107.0,108.0,109.0,110.0,111.0,112.0,  00000114
     1113.0,114.0,115.0,116.0,117.0,118.0,119.0,120.0,121.0,122.0,  00000115
     1123.0,124.0,125.0,126.0,127.0,128.0,129.0,130.0,131.0,132.0,  00000116
     1133.0,134.0,135.0,136.0,137.0,138.0,139.0,140.0,141.0,142.0,  00000117
     1143.0,144.0,145.0,146.0,147.0,148.0,149.0,150.0,151.0,152.0,  00000118
     1153.0,154.0,155.0,156.0,157.0,158.0,159.0,160.0,161.0,162.0,  00000119
     1163.0,164.0,165.0,166.0,167.0,168.0,169.0,170.0,171.0,172.0,  00000120
     1173.0,174.0,175.0,176.0,177.0,178.0,179.0,180.0,181.0,182.0,  00000121
     1183.0,184.0,185.0,186.0,187.0,188.0,189.0,190.0,191.0,192.0,  00000122
     1193.0,194.0,195.0,196.0,197.0,198.0,199.0,200.0,201.0,202.0,  00000123
     1203.0,204.0,205.0,206.0,207.0,208.0,209.0,210.0,211.0,212.0,  00000124
```

```
      1213.0,214.0,215.0,216.0,217.0,218.0,219.0,220.0,221.0,222.0,     00000125
      1223.0,224.0,225.0,226.0,227.0,228.0,229.0,230.0,231.0,232.0,     00000126
      1233.0,234.0,235.0,236.0,237.0,238.0,239.0,240.0,241.0,242.0,     00000127
      1243.0,244.0,245.0,246.0,247.0,248.0,249.0,250.0,251.0,252.0,     00000128
      1253.0,254.0,255.0,256.0,257.0,258.0,259.0,260.0,261.0,262.0,     00000129
      1263.0,264.0,265.0,266.0,267.0,268.0,269.0,270.0,271.0,272.0,     00000130
      1273.0,274.0,275.0,276.0,277.0,278.0,279.0,280.0,281.0,282.0,     00000131
      1283.0,284.0,285.0,286.0,287.0,288.0,289.0,290.0,291.0,292.0,     00000132
      1293.0,294.0,295.0,296.0,297.0,298.0,299.0,300.0,301.0,302.0,     00000133
      1303.0,304.0,305.0,306.0,307.0,308.0,309.0,310.0,311.0,312.0,     00000134
      1313.0,314.0,315.0/
      READ 1, NSAM
    1 FORMAT(8I10)                                                      00000141
      DO 13 IJK=1,NSAM                                                  00000142
   60 PRINT 500
  500 FORMAT (1H1)
      PRINT 51,IJK
   51 FORMAT(14H   PASS NUMBER I3)
      READ 312, TITLE                                                   00000 36
  312 FORMAT (20A4)
      PRINT 313, TITLE                                                  00000138
  313 FORMAT(//,1X,'THIS SAMPLE IS',20A4,//)
      IDX=0                                                             00000143
      READ 2,THERM,SI,LS,R0N0P,R0N0S,GAMMA,DELTAV                                  83
    2 FORMAT (A4,6X,F10.0,I10,4F10.0)
      IF(SI.EQ.0.0)GO TO 54                                             00000 4
      GO TO 55                                                          00000179
   54 SI = 0.01                                                         00000180
   55 CONTINUE                                                          00000181
      PRINT 61                                                          00000150
   61 FORMAT(6x,3HVpF,11x,3HVSF,12x,2HVT,11x,3HVSR,11x,3HVpR)           000001
    3 IDX=IDX+1                                                         00000149
      READ 4, VPF, VSF, VT(IDX), VSR, VPR, FLAG                         00000152
    4 FORMAT(8F10.0)                                                    00000153
      PRINT 62, VPF, VSF, VT(IDX), VSR, VPR                             00000154
   62 FORMAT(1x, 5(F11.4,3x))                                           00000  5
      REP(IDX)=(VPF + VPR)/(2.0*SI)                                     00000156
      RES(IDX)=(VSF + VSR)/(2.0*SI)                                     00000157
      IF (FLAG.EQ.0.0) GO TO 3                                          00000159
      IF(THERM.EQ.GE) GO TO 6                                           00000160
      IF (THERM.EQ.PTEP) GO TO 33
      IFLAG = PT                                                        00000161
      CALL PARINT(VPT, TPT, VT, T, IDX,284 , IFLAG)                     00000162
```

```
244                DO 5  I=1,IDX                                          00000163
245              5 TEMP(IJK,I)=T(I)                                       00000164
246                GO TO 8                                                00000 6
247             33 IFLAG = PTEP
248                CALL PARINT (VPTEP,TPTEP,VT,T,IDX,313,IFLAG)
249                DO 34 I = 1,IDX
250             34 TEMP(IJK,I) = T(I)
251                GO TO 8
252              6 IFLAG=GE                                               00000166
253                CALL PARINT(VGE, TGE, VT, T, IDX, 58, IFLAG)           00000167
254                DO 7  I=1,IDX                                          00000168
255              7 TEMP(IJK,I) = T(I)                                     00000169
256              8 CONTINUE                                               00000170
257                CALL PARINT(TALPHA,ALPHA,T,ALPH,IDX,23,IFLAG)
258                CALL PARINT(TDELT,DELT,T,DEL,IDX,18,IFLAG)
259                PRINT 50                                               00000171
260             50 FORMAT(1H1)                                            00000172
261                PRINT 51,IJK                                           00000173
262                PRINT 313,TITLE
263                PRINT 52,THERM                                         00000175
264             52 FORMAT(3H A ,A4,38H THERMOMETER WAS USED WITH THIS SAMPLE/)
265                PRINT 53,SI                                            00000177
266             53 FORMAT(18H SAMPLE CURRENT IS F6.3/)                    000001 7
267                PRINT 56, LS                                           00000182
268             56 FORMAT(10H THE FIRST, I3, 47H CARDS ARE TO BE USED TO DETERMINE F0 00000183
269               1RM FACTOR,/)                                          00000184
270                PRINT 502, R0N0S
271            502 FORMAT (28H THE VALUE USED FOR R0N0S IS F9.6/)
272                PRINT 503,R0N0P
273            503 FORMAT (28H THE VALUE USED FOR R0N0P IS F9.6/)
274                PRINT 504, GAMMA
275            504 FORMAT(29H THE VALUE USED FOR GAMMA IS F9.6/)
276                PRINT 505, DELTAV
277            505 FORMAT(29H THE VALUE USED FOR DELTAV ISF9.6/)
278            417 FORMAT(5X,E12.7,6X,E12.7)                              00000222
279                IF(LS.NE.0) GO TO 70
280                GO TO 416
281             70 READ 4, R0SAM, TSAM, R0PUR, TPUR                       00000191
282                PRINT 506,R0SAM,TSAM,R0PUR,TPUR
283            506 FORMAT(8H R0SAM = F10.8,2X,7HTSAM = ,F7.3,2X,8HR0PUR = ,F10.8,2X,
284               17HTPUR = ,F7.3/)
285                X = 0.0                                                00000192
286                Y = 0.0                                                00000193
```

```
      XY= 0.0                                                          00000194
      X2= 0.0                                                          00000195
      IF(LS.EQ.0) GO TO 416                                            00000196
      DO 9  I=1,LS                                                     00000197
      X = X + TEMP(IJK,I)                                              00000198
      Y = Y + RES(I)                                                   00000 99
      XY = XY + TEMP(IJK,I)*RES(I)                                     00000200
      X2 = X2 + TEMP(IJK,I)**2                                         00000201
    9 CONTINUE                                                         00000202
      DE = LS * X2 - X * X                                             00000203
      SM = (LS*XY - X*Y)/DE                                            00000204
      SB = (X2*Y - X*XY)/DE                                            00000205
      D = RGSAM/((SM*TSAM + SB)*(1.0-ALPH(I)))
      IF (IJK.GT.1)GO TO 11                                            00000207
      YP = 0.0                                                         00000208
      XYP = 0.0                                                        00000209
      DO 10 I=1,LS                                                     00000210
      YP = YP + REP(I)                                                 00000211
   10 XYP = XYP + TEMP(IJK,I)*REP(I)                                   00000212
      PM = (LS*XYP - X*YP)/DE                                          00000213
      PB = (X2*YP - X*XYP)/DE                                          00000214
      DP = RGPUR/((PM*TPUR + PB)*(1.0-ALPH(I)))
      GO TO 11                                                         00000216
  416 READ 417, D, DP                                                  00000217
   11 CONTINUE                                                         00000218
      PRINT 419                                                        00000219
  419 FORMAT (10X,'D IS', 10X,'DP IS')                                 00000220
      IF (LS.EQ.0.0)GO TO 420
      PUNCH 417, D, DP
  420 CONTINUE
      PRINT 417, D, DP                                                 00000221
      PRINT 63
   63 FORMAT(///5X,5HALLOY,5X,4HPURE,5X,6HPHONON,4X,5HFRACT,4X,5HFRACT,
     15X,4HTEMP,4X,5HDELTA,6X,7HDELTINV,3X,6HDELRHO,3X,6HRHODEL,2X,
     18HDELRGMAX,4X)
      PRINT 65
   65 FORMAT(4X,7HRESTVTY,3X,7HRESTVTY,3X,7HRESTVTY,3X,4HCORR,5X,4HCORR)
      PRINT 66
   66 FORMAT(34X,5HRESID,3X,6HPHONON/)
      NSAVE(IJK) = IDX                                                 00000226
      DO 13 I = 1,IDX                                                  00000227
      IF(TEMP(IJK,I).LT.160.) GO TO 600
      BETA(IJK,I)=5.3-(TEMP(IJK,I)-160.)*.00504
```

```
330             GO TO 601
331         600 BETA(IJK,I)=5.3**.0537*(160.-TEMP(IJK,I))
332         601 CONTINUE
333             DEL(I) = 0
334             GAMMA = 0
335             ROS(I)=D*(1.-ALPH(I))*RES(I)
336             ROP(I)=DP*(1.-ALPH(I))*REP(I)
337             IF (RONOP.GT.0.0) GO TO 603
338         602 RONOP = ROP(1)
339         603 CONTINUE
340             IF (RONOS.GT.0.0) GO TO 605
341         604 RONOS = ROS(1)
342         605 CONTINUE
343             RONOSC=3.**GAMMA*(.00415-ALPH(I))/1.3*
344         711 ROPH=ROP(I)-RONOP*(1.0 + DEL(I))
345         712 ROPHC = BETA(IJK,I)*DELTAV/1.34
346             DELTA=ROS(I)-ROPH*(1.-ROPHC)-RONOS*(1.-RONOSC)
347             IF (DELTA.NE.0.0) GO TO 900
348             DELTA =.0000001
349         900 CONTINUE
350             XINDEL=1./DELTA
351             DELRHO=DELTA/RONOS
352             RHODEL=RONOS/DELTA
353          64 FORMAT (3X,3(F8.6,2X),2(F7.4,2X),F7.3,2X,F9.6,2X,F8.2,2X,F7.5,2X,
354            1F7.2,2X,F8.5,2X,F5.2,5X,F8.5)
355             IF (XINDEL.GT.9999.99) GO TO 68
356             PRINT 64,ROS(I),ROP(I),ROPH,RONOSC,ROPHC,TEMP(IJK,I),DELTA,
357            1 XINDEL,DELRHO,RHODEL,DEL(I)
358             GO TO 13
359          68 PRINT 69,ROS(I),ROP(I),ROPH,RONOSC,ROPHC,TEMP(IJK,I),DELTA,
360            1 XINDEL,DELRHO,RHODEL,DEL(I)
361          69 FORMAT (3X,3(F8.6,2X),2(F7.4,2X),F7.3,2X,F9.6,2X,E8.2,2X,F7.5,2X,
362            1F7.2,2X,F8.5,2X,F5.2,5X,F8.5)
363          13 CONTINUE                                                    00000236
364             END                                                         00000293
```

98

SUBPROGRAMS

4MAIN F:105 F:106 F:108 9INITIAL M:D0 9READ 9I80DATA
9PRINT 9END10L 9I8LUSA 9RT80I PARINT 9RT80D 9IT80D 9DT8R
9IT8R 93CDWRIT 9ST8P

PROGRAM ALLOCATION

3DC•0	KM	3DD•0	KI	3DE•0	KH	3DF•0	GE	3E0•0	PT
3E1•0	BLANK	3E2•0	NSAM	3E3•0	IJK	3E4•0	IDX	3E5•0	THERM
3E6•0	SI	3E7•0	LS	3E8•0	RONOP	3E9•0	RONOS	3EA•0	GAMMA
3EB•0	DELTAV	3EC•0	VPF	3ED•0	VSF	3EE•0	VSR	3EF•0	VPR
3F0•0	FLAG	3F1•0	PTEP	3F2•0	IFLAG	3F3•0	I	3F4•0	ROSAM
3F5•0	TSAM	3F6•0	ROPUR	3F7•0	TPUR	3F8•0	X	3FA•0	Y
3FC•0	XY	3FE•0	X2	400•0	DE	402•0	SM	404•0	SB
406•0	D	407•0	YP	408•0	XYP	409•0	PM	40A•0	PB
40B•0	DP	40C•0	RONOSC	40D•0	ROPH	40E•0	ROPHC	40F•0	DELTA
410•0	XINDEL	411•0	DELRHO	412•0	RHODEL				
413•0	VT	477•0	REP	4DB•0	RES	53F•0	TEMP	733•0	VGE
76D•0	TGE	7A7•0	VPT	8C3•0	TPT	9DF•0	T	A43•0	NSAVE
A48•0	ROS	AAC•0	ROP	B10•0	TDELT	B22•0	DELT	B34•0	AX
D28•0	FX	F1C•0	NF	1110•0	KP	28BC•0	K	28C1•0	IP
406D•0	TALPHA	4084•0	ALPHA	409B•0	ALPH	40FF•0	BETA	42F3•0	RODELT
44E7•0	TITLE	44FB•0	VPTEP	4634•0	TPTEP	476D•0	DEL		

PROGRAM SIZE 47D1

PROGRAM END

```
      SUBROUTINE PARINT(XTABLE,YTABLE,X,Y,K,N,IFLAG)                    00000294
C                                                                       00000295
C     THIS SUBROUTINE DOES PARABOLIC INTERPOLATION                      000002 6
C     REFER...HILDEBRAND, INTRODUCTION TO NUM. ANALYSIS, P. 49          00000297
C     THE ROUTINE DOES LINEAR INTERPOLATION FOR ALL X-VALUES BETWEEN    000002
C     XTABLE(N-1) AND XTABLE(N)                                         00000299
C                                                                       00000300
      DIMENSION XTABLE(N),YTABLE(N),X(K),Y(K)                           00000301
  200 FORMAT (//10X,32H** ERROR IN SUBROUTINE PARINT **/                00000302
     1          13X, A8, 5X, I5, E15.3)                                00000303
  201 FORMAT (  13X,35HCARD OUT OF ORDER OR BAD DATA POINT  )           00000304
  202 FORMAT (  13X,29HVALUE OUTSIDE RANGE OF TABLES  )                 00000305
  203 FORMAT (//10X,46HMORE ERRORS OCCURRED - ONLY FIRST 5 ARE LISTED  )00000306
      MSG=IFLAG                                                         00000307
      IFLAG = 0                                                         00000308
      R = 1.0                                                           00000309
      IF(XTABLE(1).GT.XTABLE(2)) R=-1.                                  00000310
      JO=0                                                              00000311
      NL=N-1                                                            00000312
      I=1                                                               000003 3
      DO 1007 J=1,K                                                     00000314
 1005 IF(R*(XTABLE(I)-X(J))) 1002,1010,1006                             000003 5
 1002 IF(R*(X(J)-XTABLE(I+1))) 1003,1004,1004                           000003 6
 1010 Y(J)=YTABLE(I)                                                    00000317
      GO TO 1007                                                        000003 8
 1003 IF (I.EQ.NL) JO=1                                                 00000319
      F=1./(XTABLE(I+1)-XTABLE(I))                                      00000320
      DD=YTABLE(I)*(XTABLE(I+1)-X(J))                                   00000321
      DU=YTABLE(I+1)*(XTABLE(I)-X(J))                                   00000322
      YA=F*(DD-DU)                                                      00000323
      IF(JO.EQ.1) GO TO 1011                                            00000324
      F=1./(XTABLE(I+2)-XTABLE(I))                                      000003
      DD=YTABLE(I)*(XTABLE(I+2)-X(J))                                   00000326
      DU=YTABLE(I+2)*(XTABLE(I)-X(J))                                   00000327
      YB=F*(DD-DU)                                                      00000328
      F=1./(XTABLE(I+2)-XTABLE(I+1))                                    00000329
      DD=YA*(XTABLE(I+2)-X(J))                                          00000330
      DU=YB*(XTABLE(I+1)-X(J))                                          00000331
      Y(J)=F*(DD-DU)                                                    00000332
      GO TO 1007                                                        00000333
 1011 Y(J)=YA                                                           00000334
      GO TO 1007                                                        0000033
 1004 I=I+1                                                             00000336
```

```
44                IF(I.GT.N)GO TO 1009                                    00000337
45                GO TO 1005                                              00000338
46          1007  CONTINUE                                                00000339
47                RETURN                                                  00000340
48          C                                                             00000341
49          C     ERROR MESSAGES                                          00000342
50          C                                                             00000343
51           1006 IC=1                                                    00000344
52                IF (IFLAG .GT. 5)   GO TO 1100                          000003
53                GO TO 1101                                              00000346
54          1009 IC=2                                                     00000347
55                IF (IFLAG .GT. 5)   GO TO 1100                          00000348
56          1101 PRINT 200, MSG, J, X(J)                                  00000349
57               GO TO (1102,1103), IC                                    00000350
58          1102 PRINT 201                                                00000351
59               GO TO 1002                                               00000352
60          1103 PRINT 202                                                00000353
61               GO TO 1007                                               00000354
62          1100 PRINT 203                                                00000355
63               RETURN                                                   00000356
64               END                                                      00000357
```

SUBPROGRAMS

68

$PRINT F:105 F:106 F:108 $IODATA $BF:SG $ENDIOL $STOPN
$BF:SZ $BF:SR

PROGRAM ALLOCATION

1C4•0	PARINT	0•0	N	0•0	K	1C5•0	MSG	0•0	IFLAG
1C6•0	R	1C7•0	JG	1C8•0	NL	1C9•0	I	1CA•0	J
1CB•0	F	1CC•0	DD	1CD•0	DU	1CE•0	YA	1CF•0	YB
1D0•0	IC								

0•0	XTABLE	0•0	YTABLE	0•0	X	0•0	Y

PROGRAM SIZE 1D1

PROGRAM END

APPENDIX B

TYPICAL DATA OUTPUT

PASS NUMBER 3

THIS SAMPLE IS #7, AL+.035 A/O GA

VPF	VSF	VT	VSR	VPR
.4920	2.8690	2046.1001	2.8450	.5500
.4760	2.8480	988.2000	2.8740	.5720
.5060	2.8770	506.3000	2.8560	.5550
.5340	2.9210	175.3000	2.8990	.5870
.5850	2.9890	98.0500	2.9710	.6260
.6940	3.1870	54.4700	3.1660	.7440
.8110	3.3880	41.1700	3.3940	.8820
1.2050	3.9820	28.9700	3.9720	1.2520
1.5450	4.4090	25.1100	4.4140	1.5710
2.0830	5.0610	21.8400	5.0570	2.1090
4.2490	7.3510	16.6700	7.3520	4.2400
4.3140	7.4340	16.9600	7.4430	4.3350
7.3860	10.5290	13.8650	10.5280	7.3830
11.6540	14.7500	11.9600	14.7320	11.6500
25.7900	28.6100	9.2820	28.4200	25.3700

PASS NUMBER 3

THIS SAMPLE IS #7, AL=.035 A/O GA

A GE THERMOMETER WAS USED WITH THIS SAMPLE

SAMPLE CURRENT IS .010

THE FIRST 0 CARDS ARE TO BE USED TO DETERMINE FORM FACTOR,

THE VALUE USED FOR RONOS IS .007951

THE VALUE USED FOR RONOP IS .001424

THE VALUE USED FOR GAMMA IS .000000

THE VALUE USED FOR DELTAV IS .000006

D IS .2796698E-04 DP IS .2750701E-04

ALLOY RESTVTY	PURE RESTVTY	PHONON RESTVTY	FRACT CORR RESID	FRACT CORR PHONON	TEMP	DELTA	DELTINV	DELRHO	RHODEL	DELROMAX
.007957	.001427	.000003	.0000	.0001	3.101	.000003	.35E 06	.00036	.28E 04	.00000
.007968	.001435	.000011	.0000	.0001	4.351	.000006	.17E 06	.00072	.14E 04	.00000
.007983	.001453	.000029	.0000	.0001	5.872	.000003	.31E 06	.00041	.24E 04	.00000
.008105	.001535	.000111	.0000	.0001	9.110	.000042	.24E 05	.00531	.19E 03	.00000
.008300	.001659	.000235	.0000	.0001	11.738	.000114	8779.00	.01433	69.80	.00000
.008847	.001970	.000546	.0000	.0001	15.901	.000350	2855.12	.04405	22.70	.00000
.009444	.002319	.000895	.0000	.0001	18.820	.000598	1671.18	.07526	13.29	.00000
.011076	.003365	.001941	.0000	.0001	23.730	.001184	844.59	.14891	6.72	.00000
.012287	.004268	.002844	.0000	.0001	26.184	.001492	670.46	.18759	5.33	.00000
.014090	.005742	.004318	.0000	.0001	28.869	.001821	549.13	.22904	4.37	.00000
.020475	.011627	.010203	.0000	.0001	35.021	.002320	430.98	.29182	3.43	.00000
.020717	.011846	.010422	.0000	.0001	35.190	.002343	426.73	.29473	3.39	.00000
.029323	.020229	.018805	.0000	.0001	40.071	.002567	389.59	.32282	3.10	.00000

•041056	•031919	•030495	•0000	•0001	44•799	•002609	383•34	•32809	3•05	•00000
•079423	•070076	•068652	•0000	•0000	54•746	•002816	355•07	•35421	2•82	•00000

PASS NUMBER 4

HIS SAMPLE IS #7, AL+.03% 470 CA

VPF	VSF	VT	VS*	VPR
34.4900	37.3900	5795.0000	37.4900	34.7500
35.5000	38.2800	5866.0000	38.1000	35.3100
41.4300	44.1400	6445.0000	44.0400	41.3000
42.3800	45.0400	6526.0000	44.7400	41.9500
42.6100	45.5000	6545.0000	44.9900	42.4800
44.2100	46.5000	6701.0000	46.0000	44.2600
49.0300	51.4500	7153.0000	51.6800	49.3900
56.7300	59.1700	7772.0000	59.0500	56.8000
59.7700	62.1700	8016.0000	62.1200	59.7700
65.8100	68.1700	8491.0000	68.2000	65.9100
80.7300	82.7700	9591.5000	82.7700	80.7200
81.1800	83.1700	9621.0000	83.1500	81.1100
84.0300	86.8500	9839.0000	86.2700	84.2300
90.2200	96.1700	10258.0000	92.1800	90.4000
109.6200	108.4400	10961.0000	102.4400	109.8000
110.3700	111.9100	11585.0000	111.8300	110.3200
122.8000	127.1700	12374.0000	124.1400	122.9600
140.6300	141.5600	13445.0000	141.3500	140.3500
158.0600	158.9400	14485.0000	158.9000	158.2300
181.2500	181.6900	15780.0000	181.6400	181.2800
204.3800	204.3500	17066.0000	204.2900	204.5200
240.8600	240.2800	19004.0000	239.7700	240.3300
242.8600	242.3300	19106.0000	242.2700	242.8700
264.1600	263.3401	20222.0000	263.2300	264.2100
271.1200	270.0601	20586.0000	270.1300	271.1201
345.1201	343.0701	24363.0000	342.9800	345.2000
380.4900	377.8101	26138.0000	377.7400	380.5601
473.0500	469.1101	30755.0000	469.1001	473.1799
480.8799	476.7700	31149.0000	476.7400	481.0200
636.0601	629.6699	38283.0000	629.6799	636.2700
822.0400	812.0500	48043.0000	812.8899	822.2200
925.7800	916.2200	53163.0000	916.1699	926.1101
960.5400	949.5400	54863.0000	949.5000	960.3500
970.8201	959.6599	55371.0000	959.6201	971.2000
979.5601	968.3000	55813.0000	968.2600	979.9800

987•8701 976•4299 56218•0000 976•3999 988•2700

PASS NUMBER 4

THIS SAMPLE IS #7, AL+.035 A70 GA

A PT THERMOMETER WAS USED WITH THIS SAMPLE

SAMPLE CURRENT IS .010

THE FIRST 0 CARDS ARE TO BE USED TO DETERMINE FORM FACTOR,

THE VALUE USED FOR RONOS IS .007951

THE VALUE USED FOR RONOP IS .001424

THE VALUE USED FOR GAMMA IS .000000

THE VALUE USED FOR DELTAV IS .000006

D IS .2796698E-04 DP IS .2750701E-04

ALLOY RESTVTY	PURE RESTVTY	PHONON RESTVTY	FRACT CORR RESID	FRACT CORR PHONON	TEMP	DELTA	DELTINV	DELRHO	RHODEL	DELROMAX
.104284	.094843	.093419	.0000	.0000	59.723	.002909	343.72	.36591	2.73	.00000
.106304	.096994	.095570	.0000	.0000	60.063	.002778	359.97	.34939	2.86	.00000
.122809	.113324	.111899	.0000	.0000	62.805	.002953	338.63	.37141	2.69	.00000
.125037	.115515	.114091	.0000	.0000	63.185	.002990	334.48	.37601	2.66	.00000
.126026	.116557	.115133	.0000	.0000	63.274	.002937	340.44	.36943	2.71	.00000
.130637	.121187	.119763	.0000	.0000	64.005	.002917	342.80	.36689	2.73	.00000
.144468	.134901	.133477	.0000	.0000	66.117	.003035	329.54	.38166	2.62	.00000
.164652	.155519	.154095	.0000	.0000	68.963	.002599	384.79	.32686	3.06	.00000
.173107	.163753	.162329	.0000	.0000	70.082	.002820	354.65	.35463	2.82	.00000
.189935	.180441	.179017	.0000	.0000	72.252	.002959	337.96	.37214	2.69	.00000
.236572	.221177	.219753	.0000	.0000	77.251	.002859	349.78	.35956	2.78	.00000
.231659	.222328	.220904	.0000	.0000	77.384	.002794	357.85	.35146	2.85	.00000
.240296	.230508	.229084	.0000	.0000	78.370	.003251	307.56	.40893	2.45	.00000

.256778	.247445	.246021	.0000	.0000	80.261	.002796	357.65	.35166	2.84	.00000
.285383	.275949	.274525	.0000	.0000	83.431	.002896	345.36	.36418	2.75	.00000
.311662	.302358	.300934	.0000	.0000	86.242	.002765	361.61	.34780	2.88	.00000
.350079	.336718	.335294	.0000	.0000	89.795	.006821	146.60	.85792	1.17	.00000
.394119	.384992	.383568	.0000	.0000	94.634	.002584	386.93	.32504	3.08	.00000
.442803	.433396	.431972	.0000	.0000	99.332	.002863	349.25	.36011	2.78	.00000
.506216	.496794	.495370	.0000	.0000	105.203	.002877	347.58	.36184	2.76	.00000
.569389	.560381	.558957	.0000	.0000	111.052	.002462	406.19	.30963	3.23	.00000
.668695	.659534	.658110	.0000	.0000	119.918	.002613	382.74	.32860	3.04	.00000
.675319	.665761	.664337	.0000	.0000	120.387	.003009	332.32	.37846	2.64	.00000
.733849	.724274	.722850	.0000	.0000	125.521	.003025	330.53	.38051	2.63	.00000
.752878	.743305	.741881	.0000	.0000	127.200	.003022	330.90	.38008	2.63	.00000
.956422	.946546	.945122	.0000	.0000	144.733	.003323	300.92	.41796	2.39	.00000
1.053465	1.043680	1.042255	.0000	.0000	153.038	.003233	309.33	.40658	2.46	.00000
1.308667	1.298146	1.296721	.0000	.0000	174.813	.003965	252.20	.49870	2.01	.00000
1.330055	1.319691	1.318266	.0000	.0000	176.682	.003809	262.55	.47903	2.09	.00000
1.757953	1.746861	1.745437	.0000	.0000	213.417	.004527	220.90	.56935	1.76	.00000
2.271687	2.259640	2.258215	.0000	.0000	258.076	.005474	182.69	.68845	1.45	.00000
2.560342	2.546420	2.544995	.0000	.0000	283.178	.007345	136.15	.92378	1.08	.00000
2.655433	2.642634	2.641210	.0000	.0000	291.591	.006220	160.78	.78225	1.28	.00000
2.683886	2.671021	2.669596	.0000	.0000	294.070	.006285	159.10	.79052	1.26	.00000
2.708184	2.695251	2.693826	.0000	.0000	296.254	.006354	157.38	.79916	1.25	.00000
2.731063	2.718207	2.716783	.0000	.0000	298.256	.006275	159.36	.78920	1.27	.00000

APPENDIX C

ANALYSIS OF ERRORS

ANALYSIS OF ERRORS[1]

Resistivity Measurements

For most samples, the room temperature resistivity was calculated by substituting Equation 4.2 into Equation 4.1 to get

$$\rho = \frac{mR}{d\ell_o^2} \qquad C.1$$

where m is the mass of a wire sample of length ℓ_o, resistance R and density d. Table C.1 lists the variable, the assumed standard deviations, s, approximate magnitudes, and the fractional standard deviations, δ of the variables.

TABLE C-1.--Standard deviations for measurements using Equation C.1.

Variable (units)	Approximate Magnitude	s	δ
m (grams)	.10000[a]	.00001	10^{-4}
m (grams)	.050000[b]	.000001	2×10^{-5}
R (μ ohms)[c]	.50000	.00007	1.4×10^{-4}
d (gm/cm^3)	2.6984[d]	.0003	10^{-4}
ℓ_o (cm)	80.000	.008	10^{-4}

[a]When using Mettler B-6 semi-micro balance.

[b]When using Cahn microbalance.

[c]Measured by comparing voltage drop with that across a 10 ohm, .005% standard resistor.

[d]The value for pure aluminum.

The density of an alloy was calculated using

$$d\ (\text{alloy}) = 2.6984 + \frac{\partial d}{\partial c}\, c. \qquad \text{C.2}$$

where c is the alloy concentration, and $\partial d/\partial c$ was calculated from data tabulated by Pearson (27). The data for $\partial d/\partial c$ values is reliable to about 5%. So, assuming the reliability of c is 1% and since for copper, zinc and gallium as solutes, $\partial d/\partial c \simeq .01$ gm/cm^3-at%, a one atomic per cent alloy has a fractional standard deviation for the density of about 3×10^{-4}. Using these data, the anticipated fractional standard deviation for the room temperature resistivity of a dilute alloy is

$$\delta_\rho = (1^2 + 1^2 + (1.4 + 2)^2)^{1/2} \times 10^{-4} \qquad \text{C.3a}$$

$$\simeq .04\%. \qquad \text{C.3b}$$

And for a concentrated alloy,

$$\delta_\rho = (1^2 + 3^2 + (1.4 + 2)^2)^{1/2} \times 10^{-4} \qquad \text{C.4a}$$

$$\simeq .05\%. \qquad \text{C.4b}$$

The errors in measurement of ℓ_o and R were assumed to be completely correlated, and as such were added linearly. The former estimate is more appropriate for the concentrated magnesium alloys, since $\partial d/\partial c$ is $<<$ .01 for magnesium alloys.

The analysis of errors for the cases in which Equation 4.7 was used is more easily done if the denominator of Equation 4.7 is rewritten such that

$$\rho = \frac{m}{d\, n\ell_i \frac{1}{n} \sum_{i=1}^{n} \frac{\ell_i}{R_i}}. \qquad C.5$$

Now since $n\ell_i = \ell_o$ as defined for Equation C.1, the fractional standard deviations for all terms except the summation are the same as in the above case. The fractional standard deviation of $n\ell_i$ was kept the same as for ℓ_o by "leap-frogging" the potential probes in the formation of the separate ℓ_i. The standard deviation of ℓ_i is the same as for ℓ_o, so the fractional standard deviation for the summation is

$$\delta_\Sigma = n^{-1/2} (n\delta_\ell + \delta_R), \qquad C.6$$

noting again that R_i and ℓ_i are correlated. Assuming the correlation between ℓ_o and the summation to be weak, for n = 6 (the usual case), we have

$$\delta_\rho = (1^2 + 1^2 + 1^2 + (2.5 + \frac{1.4}{2.5})^2)^{1/2} \times 10^{-4} \qquad C.7a$$

$$\simeq .04\%. \qquad C.7b$$

If n had to be chosen much greater than 6 or 7, another wire sample was used.

The analysis

Equation 4.7 was

nator of Equation

Now since n_i

tional standard

tion are the

standard deviation

"leap-frogging"

the separate

as for t_0,

summation is

C.6

noting again that

correlation between

$n = 6$ (the usual case).

$$\delta_g^2 = (t_1^2 + t_2^2 + t_3^2 + (2r_{12} + \frac{1}{2}r_{13} + \frac{1}{2}r_{23})t_1t_2 + \ldots$$ C.7a

C.7b

If n had to be chosen much greater than 6 or 7, another

wise sample was used.

Temperature-Dependent Resistivity

The resistance of the wire samples as mounted in the cryostat was determined by voltage comparison with a standard resistor. Since only the resistance and the room temperature resistivity enter into calculations of the temperature-dependent resistivity, the fractional standard deviation for errors in the temperature-dependent resistivity were assumed to be ≃ .05%. Table C-2 compares the room temperature resistivity reported by other investigators with that measured in this study.

TABLE C-2.--Phonon resistivity of aluminum at 273.16°K.

Investigator	ρ (μΩ-cm)
This study	2.429
This study (two-band correction)	2.427
Seth and Woods (11)	2.429
a	2.44

[a]L.A. Hall, Survey of Electrical Resistivity Measurements on 16 Pure Metals in the Temperature Range 0 to 273°K (U.S. Natl. Bur. Std. Technical Note 365, 1968).

Errors in measurement of temperature were .01°K in the range of the platinum resistance thermometer and decreasing from .01°K to .001°K at 4°K for the germanium resistance thermometer range.

Errors in Calculations of Deviations from Matthiessen's Rule

Deviations from the MR were calculated using Equation 1.5. We examine the error at 295°K, 70°K, and in the very low temperature region.

At 295°K, ± .05% of ρ_{ph} is ± .001 μΩ-cm and the error in the term, $\rho_A - \rho_o$, ranges from ± .001 μΩ-cm for dilute alloys to ± .002 μΩ-cm for the concentrated alloys. Thus errors in Δ(295) are about ± .002 μΩ-cm. Now from Figure 16 it may be seen that

$$\frac{\rho_o}{\Delta} = 1 + 14\ (\mu\Omega\text{-cm})^{-1}\ \rho_o. \qquad C.8$$

The fractional error in Δ/ρ_o is given by

$$\frac{\pm\ .002\mu\Omega cm}{\rho_o}\ \frac{\rho_o}{\Delta} = \frac{.002\mu\Omega cm}{\rho_o}\ [1 + 14(\mu\Omega cm)^{-1}\rho_o]. \qquad C.9$$

For the most dilute alloy, ρ_o = .008 μΩ-cm, so the fractional error is 25%. For the most concentrated alloy, ρ_o = .76 μΩ-cm, so the fractional error is 3% which is the order of magnitude of the agreement with Seth and Woods (11) indicated in Figure 16. As derived in Equation 4.20, the errors due the pressure corrections may be as large as 5%.

At 70°K, Δ is as large or larger than it was at 295°K. However ρ_{ph} has fallen to about one-sixth of its room temperature value. The net result is that Δ has

error bars from 3% for the concentrated alloys to about 8% for the dilute alloys.

At low temperatures, Equation 5.4 shows that

$$\Delta = cT^3. \qquad \text{C.10}$$

Since this is in the region where ρ_{ph} is increasingly negligible with decreasing temperature, one can calculate the temperature at which Δ has an anticipated error of 100% as the temperature where

$$\rho_A - \rho_o = \Delta = 5 \times 10^{-4}\ \rho_o, \qquad \text{C.11}$$

since this means $\rho_A - \rho_o$ equals the standard deviation of both. Solving for T from C.11 and C.10, we have

$$T(100\%) = \left[\frac{5 \times 10^{-4}\ \rho_o}{c}\right]^{1/3} \qquad \text{C.12}$$

For $\rho_o = .10\ \mu\Omega\text{cm}$, $c = 3 \times 10^{-7}\ \mu\Omega\text{cm}/^\circ\text{K}^3$, so

$$T(100\%) = \left[\frac{5 \times 10^{-4} \times 10^{-1}}{3 \times 10^{-7}}\right]^{1/3} {}^\circ\text{K} \qquad \text{C.13a}$$

$$\simeq 5^\circ\text{K}. \qquad \text{C.13b}$$

The error decreases to the values discussed for 70°K as T^{-3}.

---

[1] Y. Beers, Introduction to the Theory of Errors (Addison-Wesley, Reading, Massachusetts, 1958).